Meteoritics & Planetary Science 37, 155–182 (2002)
Available online at http://www.uark.edu/meteor

Plagioclase-rich chondrules in the reduced CV chondrites: Evidence for complex formation history and genetic links between calcium-aluminum-rich inclusions and ferromagnesian chondrules

ALEXANDER N. KROT[1]*, IAN D. HUTCHEON[2] AND KLAUS KEIL[1]

[1]Hawai'i Institute of Geophysics and Planetology, School of Ocean and Earth Science and Technology, University of Hawai'i at Manoa, Honolulu, Hawai'i 96822, USA
[2]Lawrence Livermore National Laboratory, L-231, P.O. Box 808, Livermore, California 94551, USA
*Correspondence author's e-mail address: sasha@higp.hawaii.edu

(Received 2001 June 6; accepted in revised form 2001 October 31)

Abstract–Plagioclase-rich chondrules (PRCs) in the reduced CV chondrites Efremovka, Leoville, Vigarano and Grosvenor Mountains (GRO) 94329 consist of magnesian low-Ca pyroxene, Al-Ti-Cr-rich pigeonite and augite, forsterite, anorthitic plagioclase, FeNi-metal-sulfide nodules, and crystalline mesostasis composed of silica, anorthitic plagioclase and Al-Ti-Cr-rich augite. The silica grains in the mesostases of the CV PRCs are typically replaced by hedenbergitic pyroxenes, whereas anorthitic plagioclase is replaced by feldspathoids (nepheline and minor sodalite). Some of the PRCs contain regions that are texturally and mineralogically similar to type I chondrules and consist of forsterite, low-Ca pyroxene and abundant FeNi-metal nodules. Several PRCs are surrounded by igneous rims or form independent compound objects. Twelve PRCs contain relic calcium-aluminum-rich inclusions (CAIs) composed of anorthite, spinel, high-Ca pyroxene, ±forsterite, and ±Al-rich low-Ca pyroxene. Anorthite of these CAIs is generally more heavily replaced by feldspathoids than anorthitic plagioclase of the host chondrules. This suggests that either the alteration predated formation of the PRCs or that anorthite of the relic CAIs was more susceptible to the alteration than anorthitic plagioclase of the host chondrules. These observations and the presence of igneous rims around PRCs and independent compound PRCs suggest that the CV PRCs may have had a complex, multistage formation history compared to a more simple formation history of the CR PRCs.

Relatively high abundances of moderately-volatile elements such as Cr, Mn and Si in the PRCs suggests that these chondrules could not have been produced by volatilization of ferromagnesian chondrule precursors or by melting of refractory materials only. We infer instead that PRCs in carbonaceous chondrites formed by melting of the reduced chondrule precursors (magnesian olivine and pyroxene, FeNi-metal) mixed with refractory materials (relic CAIs) composed of anorthite, spinel, high-Ca pyroxene, and forsterite. The mineralogical, chemical and textural similarities of the PRCs in several carbonaceous chondrite groups (CV, CO, CH, CR) and common presence of relic CAIs in these chondrules suggest that PRCs may have formed in the region(s) intermediate between the regions where CAIs and ferromagnesian chondrules originated.

INTRODUCTION

The short-lived radionuclide ^{26}Al ($t_{1/2} \approx 0.73$ Ma) was present in the nebular regions where calcium-aluminum-rich inclusions (CAIs) and chondrules formed and has important implications for understanding the chronology of the early solar system. Based on the correlated occurrences (absence/presence) of ^{26}Al and ^{41}Ca ($t_{1/2} \approx 0.1$ Ma) in CAIs, it was concluded that these radionuclides had a stellar origin and were injected into the protosolar cloud during its collapse (Sahijpal *et al.*, 1998; Goswami and Vanhala, 2000). Sahijpal *et al.* (1998) suggested that this process would probably result in a uniform distribution of ^{26}Al in the CAI- and chondrule-forming regions, although Vanhala and Boss (2000) and Boss (2001) pointed out that local heterogeneities could be produced as well.

Most CAIs from different chondrite groups have the "canonical" $(^{26}Al/^{27}Al)_I$ ratio of about (4–5) × 10^{-5}, whereas chondrules analyzed so far have $(^{26}Al/^{27}Al)_I$ ratios of $<1.5 \times 10^{-5}$ (Lee *et al.*, 1976; Hutcheon and Hutchison, 1989; Goswami *et al.*, 1994; MacPherson *et al.*, 1995; Russell *et al.*, 1996, 1997; Srinivasan *et al.*, 1996a,b; Mostefaoui *et al.*, 1999; Kita *et al.*, 2000; McKeegan *et al.*, 2000a; Ito *et al.*, 2000;

Prelude preprint MS#4565

Hutcheon *et al.*, 2000; Huss *et al.*, 2001). Based on these observations and the assumption that ^{26}Al was initially homogeneously distributed in the nebular regions from which both CAIs and chondrules formed, it is generally inferred that chondrules formed 2–5 Ma after CAIs (*e.g.*, Podosek and Cassen, 1994; MacPherson *et al.*, 1995; Russell *et al.*, 1996, 1997; Mostefaoui *et al.*, 1999; Goswami and Vanhala, 2000; Kita *et al.*, 2000; Wadhwa and Russell, 2000; Huss *et al.*, 2001).

This chronological interpretation has been questioned recently by several research groups (*e.g.*, Shu *et al.*, 1996, 1997, 2001; Wood, 1996, 1998a,b; McKeegan *et al.*, 1998, 2000a,b; Krot *et al.*, 1999; Guan *et al.*, 2000a,b; Fagan *et al.*, 2000a,b), who suggested that CAIs and chondrules may have formed contemporaneously in spatially separated and isotopically distinct reservoirs. In the x-wind model, CAIs and chondrules formed at the inner edge of the accretionary disk, near the early Sun, and were subsequently transported by a magneto-centrifugally driven stellar wind out to planetary distances, where accretion with low-temperature, fine-grained matrix material took place (*e.g.*, Shu *et al.*, 1996, 1997, 2001). According to this model, ^{26}Al was produced locally, in the solar nebula, by irradiation; lower abundance of ^{26}Al in chondrules compared to CAIs resulted from shielding of chondrules or chondrule precursors from irradiation by nebular gas (Gounelle *et al.*, 2001). If this model is correct, then the chronological significance of the ^{26}Al-^{26}Mg systematics for understanding the time difference between CAI and chondrule formation might be weakened, although the ^{26}Al-^{26}Mg systematics will remain valid for dating the complex histories of the CAIs (*e.g.*, MacPherson and Davis, 1993; Hsu *et al.*, 2000).

In order to understand the genetic relationship between CAIs and chondrules and the distribution ^{26}Al in the chondrule-forming region(s), we initiated systematic study of chondrules suitable for Al-Mg isotopic studies in primitive carbonaceous chondrites (CR, CH, reduced CV, and the ungrouped meteorites Adelaide and Acfer 094) using x-ray elemental technique, scanning electron microscope (SEM), electron probe microanalysis (EPMA) and ion microprobe. We discovered that all these meteorites contain a population of chondrules which are rich in anorthitic plagioclase (plagioclase-rich chondrules or PRCs) and commonly associated with CAIs (Krot *et al.*, 1999; Krot, 2000; Hutcheon *et al.*, 2000; Marhas *et al.*, 2000). Plagioclase-rich chondrules are magnesian chondrules composed of crystalline anorthitic plagioclase, Al-rich low-Ca and high-Ca pyroxenes, forsteritic olivine and crystalline silica-anorthite-pyroxene mesostasis. These chondrules are commonly associated with relic CAIs. These features make them ideal for understanding both the genetic relationship between CAIs and chondrules and the distribution of ^{26}Al in the chondrule-forming region. In our recent paper (Krot and Keil, 2002), we described the mineralogy and petrography of PRCs in the CR and CH carbonaceous chondrites. Here we describe the mineralogy and petrography of PRCs in the reduced CV chondrites Efremovka, Leoville, Vigarano and Grosvenor Mountains (GRO) 93429 and discuss their origin. We show that PRCs in the reduced CV chondrites share many common mineralogical features with those in CR and CH chondrites, including common presence of relic CAIs, but appear to have experienced a more complicated formation history, including alteration and remelting. Studies of Al-Mg-isotope systematics of the CR, CH and CV PRCs will be reported in a companion paper.

ANALYTICAL PROCEDURES

Forty-one polished thin sections of the reduced CV chondrites Efremovka, Leoville, Vigarano, and GRO 94329 (Table 1) were studied to search for Al-rich chondrules using optical microscopy, backscattered electron (BSE) imaging, x-ray elemental mapping, and quantitative EPMA. To identify the Al-rich chondrules, x-ray elemental maps with a resolution of 2–5 μm/pixel were acquired using five spectrometers of the Cameca microprobe at 15 kV accelerating voltage, 50–100 nA beam current and about 1–2 μm beam size. The elemental maps in Mg, Ca, and Al Kα were combined using an RGB-color scheme and ENVI software. BSE images were obtained with a Zeiss DSM-962 SEM using a 15 kV accelerating voltage and 1–2 nA beam current. Electron probe microanalyses were performed with a Cameca SX-50 electron microprobe using a 15 kV accelerating voltage, 10–20 nA beam current, beam size of about 1–2 μm and wavelength dispersive x-ray spectroscopy. For each element, counting times on both peak and background were 30 s (10 s for Na and K). Matrix effects were corrected using PAP procedures. The element detection limits with the Cameca SX-50 were (in wt%): SiO_2, Al_2O_3, MgO, 0.03; TiO_2, CaO, K_2O, 0.04; Na_2O, Cr_2O_3, 0.06; MnO, 0.07; FeO, 0.08.

RESULTS

General Mineralogy and Petrography of Plagioclase-Rich Chondrules

Plagioclase-rich chondrules are common in the reduced CV chondrites studied; more than 100 PRCs were identified (Table 1). These chondrules are magnesium-rich (Fa and Fs contents of olivine and pyroxenes, respectively, <5 mol%) and typically have porphyritic olivine (PO), porphyritic olivine-pyroxene (POP) and porphyritic pyroxene (PP) textures; barred olivine (BO) textures are rare (Figs. 1 and 2). Some of the PRCs are surrounded by a shell of low-Ca pyroxene (Fig. 2a,b), similar to what has been observed for many type I chondrules (Jones and Scott, 1989).

PRCs in the reduced CV chondrites typically consist of low-Ca pyroxene and olivine phenocrysts, lath-shaped anorthitic plagioclase, FeNi-metal/sulfide nodules, interstitial pigeonite overgrown by augite, and crystalline mesostasis composed of anhedral grains of anorthitic plagioclase, silica, and augite (Fig. 1). The coarse plagioclase grains typically contain thin sub-parallel lamellae of nepheline, suggesting that replacement

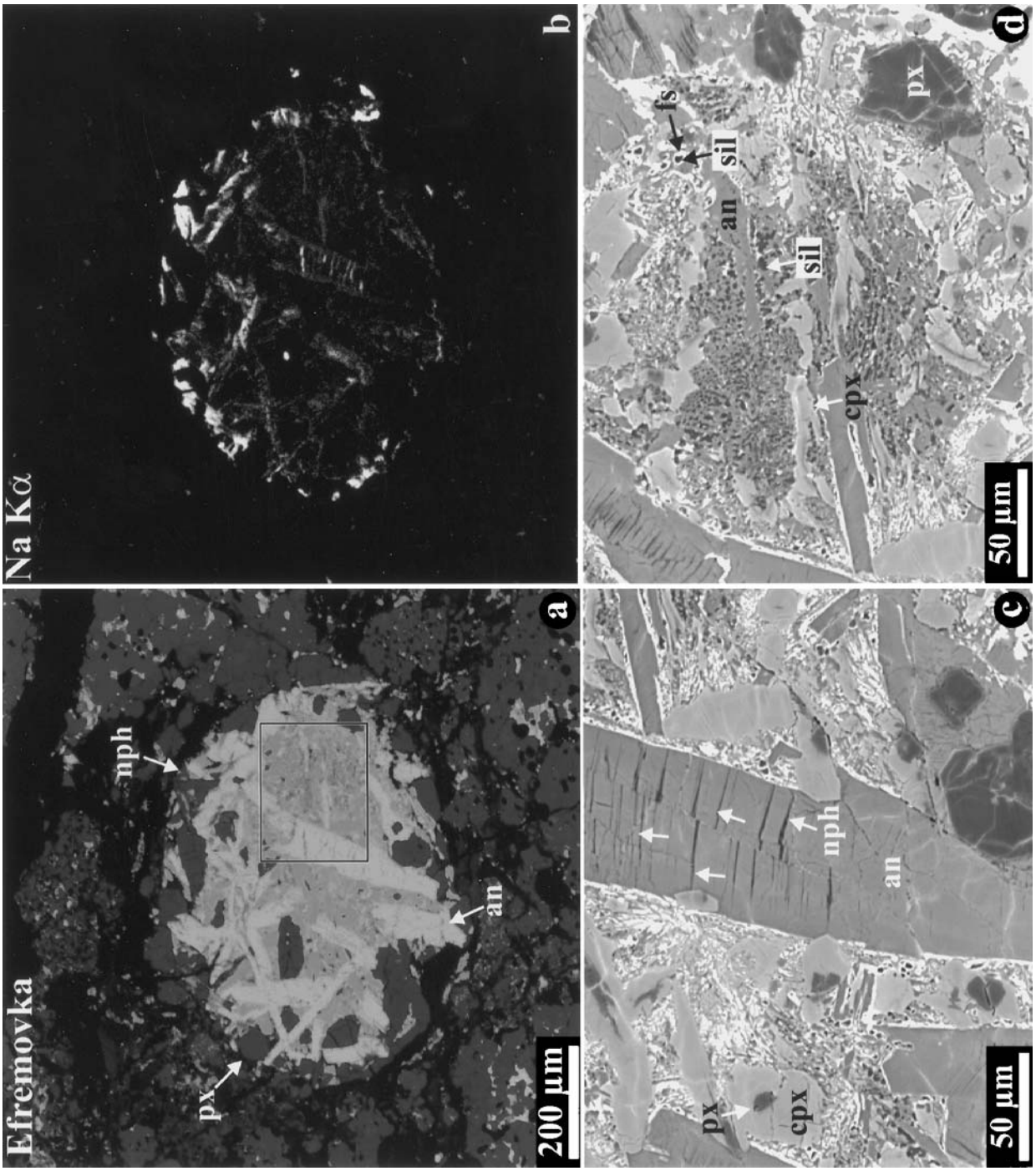

FIG. 1. Combined x-ray elemental map in Mg, Ca and Al Kα (a), elemental map in Na Kα x-rays (b) and BSE images (c, d) of PRC #2 in Efremovka (2 = number of the polished thin section). Region outlined in (a) is shown in detail in (c) and (d). The chondrule consists of low-Ca pyroxene phenocrysts (px) overgrown by high-Ca pyroxene (cpx), prismatic crystals of anorthitic plagioclase (an) and crystalline mesostasis composed of plagioclase, silica (sil, black) and high-Ca pyroxene; silica is replaced by Ca,Fe-rich pyroxene (fs, bright white). Plagioclase is partly replaced by nepheline (nph).

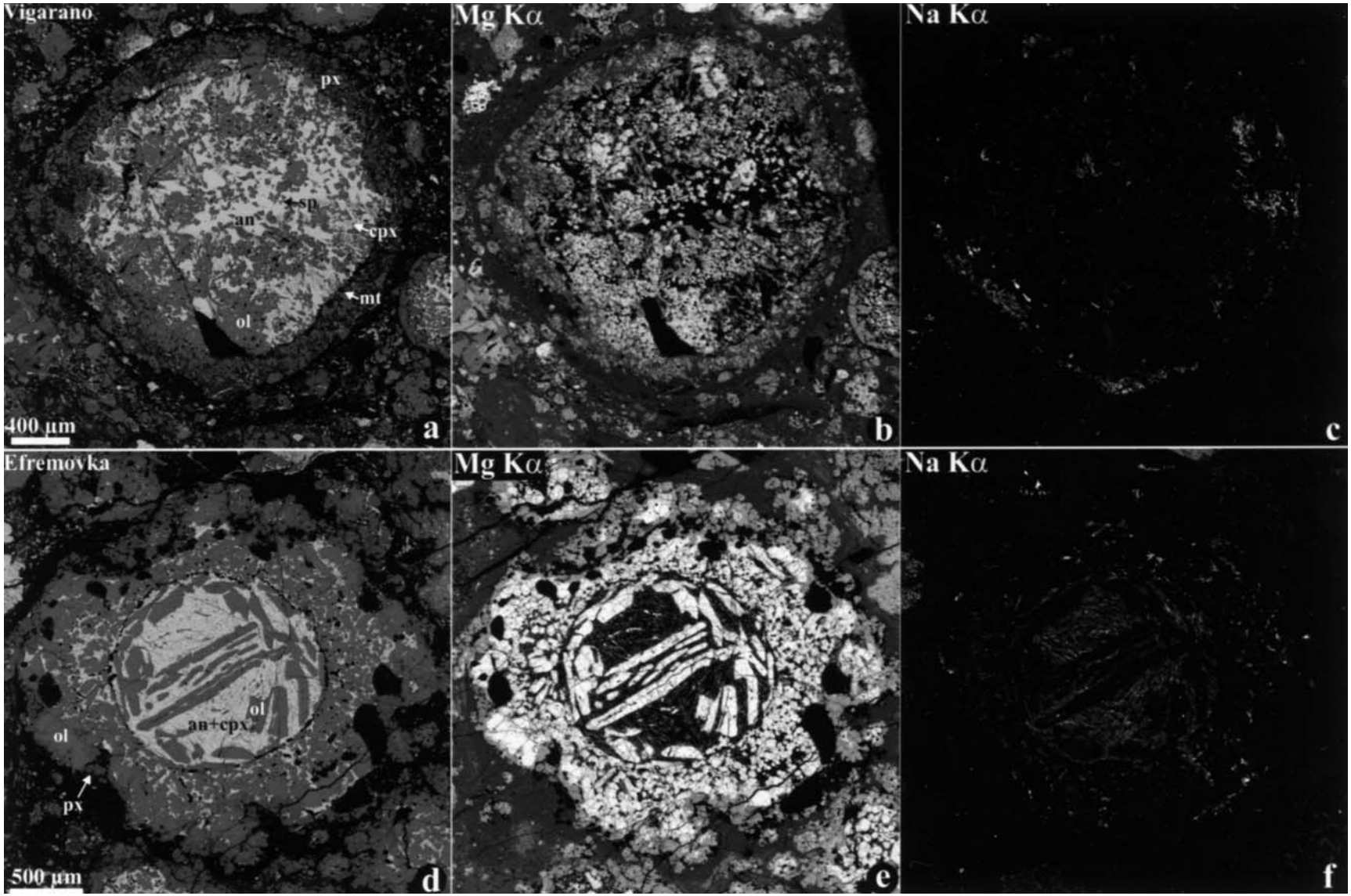

FIG. 2. Combined x-ray elemental maps (a, d, g, j), and elemental maps in Mg (b, e, h, k) and Na Kα x-rays (c, f, i, l) of the PRCs #3 (a–c) and #2 (g–i) in Vigarano (UH 63), #2 (d–f) in Efremovka (E 105) and #5 (j–l) in Efremovka (E 103-a). (a–c) The chondrule consists of lath-shaped anorthitic plagioclase, elongated grains of low-Ca pyroxene overgrown by high-Ca pyroxene and forsterite regions with abundant FeNi-metal nodules; minor spinel (sp) occurs as inclusions in plagioclase. Chondrule is surrounded by a low-Ca pyroxene shell. (d–f) The chondrule consists of elongated forsterite grains surrounded by fine-grained anorthite, high-Ca pyroxene and mesostasis. Chondrule is surrounded by a thick igneous rim having porphyritic texture and composed of forsterite, low-Ca pyroxene, abundant FeNi-metal nodules (black) and mesostasis.

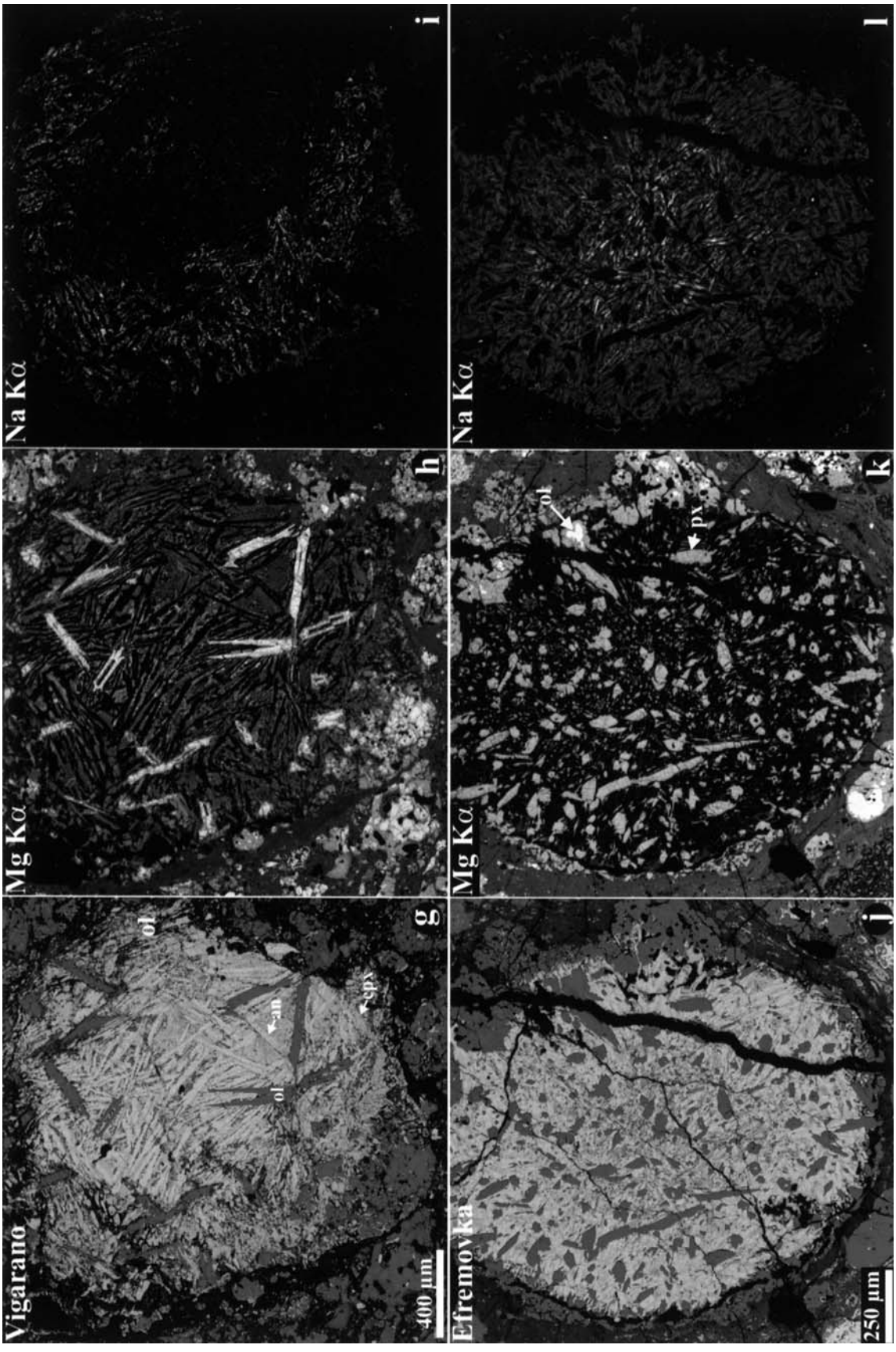

FIG. 2. *Continued.* Combined x-ray elemental maps (a, d, g, j), and elemental maps in Mg (b, e, h, k) and Na Kα x-rays (c, f, i, l) of the PRCs #3 (a–c) and #2 (g–i) in Vigarano (UH 63), #2 (d–f) in Efremovka (E 105) and #5 (j–l) in Efremovka (E 103-a). (g–i) The chondrule consists of skeletal forsterite grains, lath-shaped anorthitic plagioclase and elongated grains of low-Ca pyroxenes overgrown by high-Ca pyroxenes; forsterite-low-Ca pyroxene region with abundant inclusions of FeNi-metal nodules occurs in the peripheral portion of the chondrule. (j–l) The chondrule consists of elongated phenocrysts of low-Ca pyroxene, lath-shaped anorthitic plagioclase, interstitial high-Ca pyroxene and mesostasis; coarse low-Ca pyroxene grains poikilitically enclosing forsterite occur in the chondrule periphery. Plagioclase in the chondrule core is partly replaced by nepheline.

is crystallographically controlled by the host plagioclase (Fig. 1c,d). Plagioclase grains along the chondrule peripheries are typically more extensively replaced by nepheline (Figs. 1b and 2c,f,i). In one of the PRCs, however, feldspathoids (nepheline and minor sodalite) are preferentially concentrated in the chondrule core (Fig. 2l). The silica grains in the mesostases of many PRCs are replaced by ferrosilite-hedenbergitic pyroxene (Fig. 1c,d). The representative chemical compositions of the primary and secondary minerals in these PRCs are listed in Tables 2–7 and illustrated in Figs. 3–8.

TABLE 1. List of thin sections of CV chondrites studied.

Chondrite	Polished section	Chd no.
Vigarano	KF-1	1
Vigarano	UH 63	4
Vigarano	UH 35	4
Vigarano	USNM 6295-3	0
GRO 93429	8	1
Leoville	UH 122	11
Leoville	1	4
Leoville	2	7
Leoville	3	3
Leoville	4	2
Efremovka	1	5
Efremovka	n1	3
Efremovka	2	13
Efremovka	n2	9
Efremovka	5	4
Efremovka	5b	3
Efremovka	3-7-2	1
Efremovka	3-13-1	2
Efremovka	6-3-3	3
Efremovka	8-7-22	5
Efremovka	E 42	0
Efremovka	E 44-n	0
Efremovka	E 101-b	2
Efremovka	E 36	0
Efremovka	E38	0
Efremovka	E 44	2
Efremovka	E 44-c	1
Efremovka	E 40	0
Efremovka	E 48	1
Efremovka	E 48-c	1
Efremovka	E 54	0
Efremovka	E 59	1
Efremovka	E 60	0
Efremovka	E 65-66	3
Efremovka	E 102	2
Efremovka	E 103-a	6
Efremovka	E 103-b	4
Efremovka	E 105	1
Efremovka	E 106	0
Efremovka	E 107	0
Efremovka	E 104	1

Abbreviation: Chd no. = number of PRCs identified.

Pyroxenes range in composition from enstatite (Wo_{1-5}) to pigeonite (Wo_{5-10}) to augite (Wo_{30-40}); diopsidic pyroxenes (Wo_{45-50}) are virtually absent (Fig. 3a). Most pyroxenes are FeO-poor (Fs_{1-5}); a few analyses with Fs contents >5–10 mol% are from fine-grained mesostases and possibly due to overlap of the electron beam with secondary Fe-rich minerals (ferrous olivine and ferrosilite), commonly observed in the CV PRCs (Table 7; Fig. 1d). The low-Ca and high-Ca pyroxenes in PRCs are characterized by high TiO_2, Cr_2O_3, Al_2O_3 and MnO (Tables 2 and 3; Fig. 4). All the grains of low-Ca pyroxene with high Al_2O_3 are located within relic CAIs (see section "Refractory

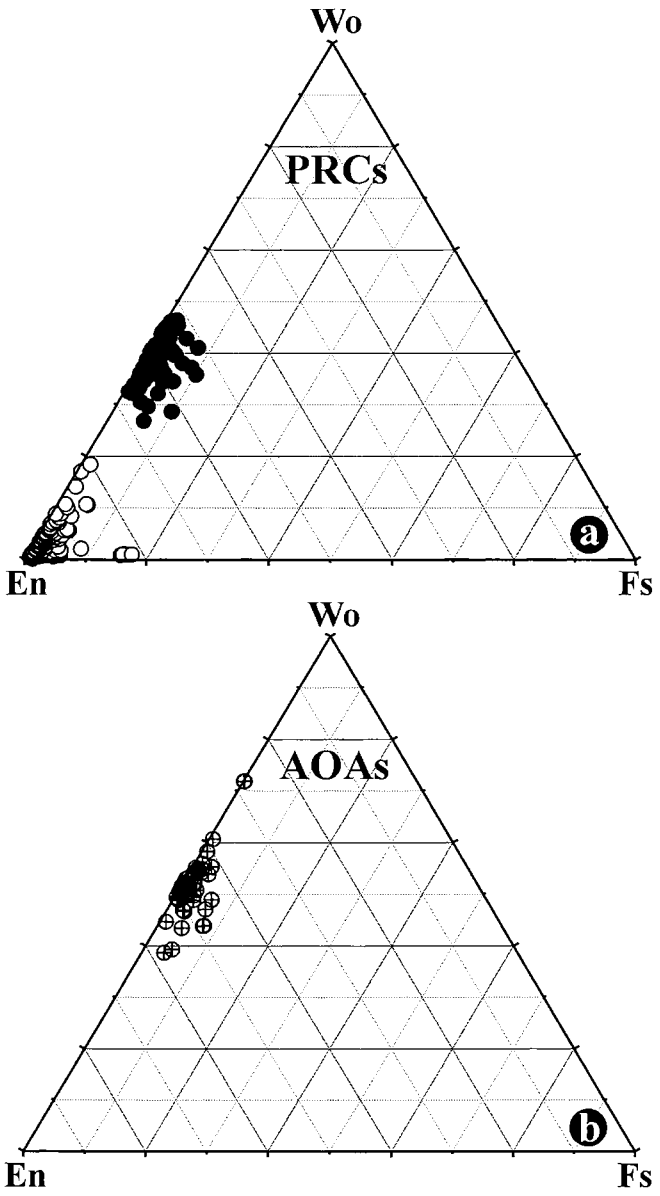

FIG. 3. Compositions of pyroxenes in the PRCs (a) and AOAs (b) in the reduced CV chondrites. Data for pyroxenes in AOAs are from Komatsu *et al.* (2001). Pyroxenes in PRCs range in composition from low-Ca pyroxene to pigeonite to augite; pyroxenes in AOAs have diopsidic compositions.

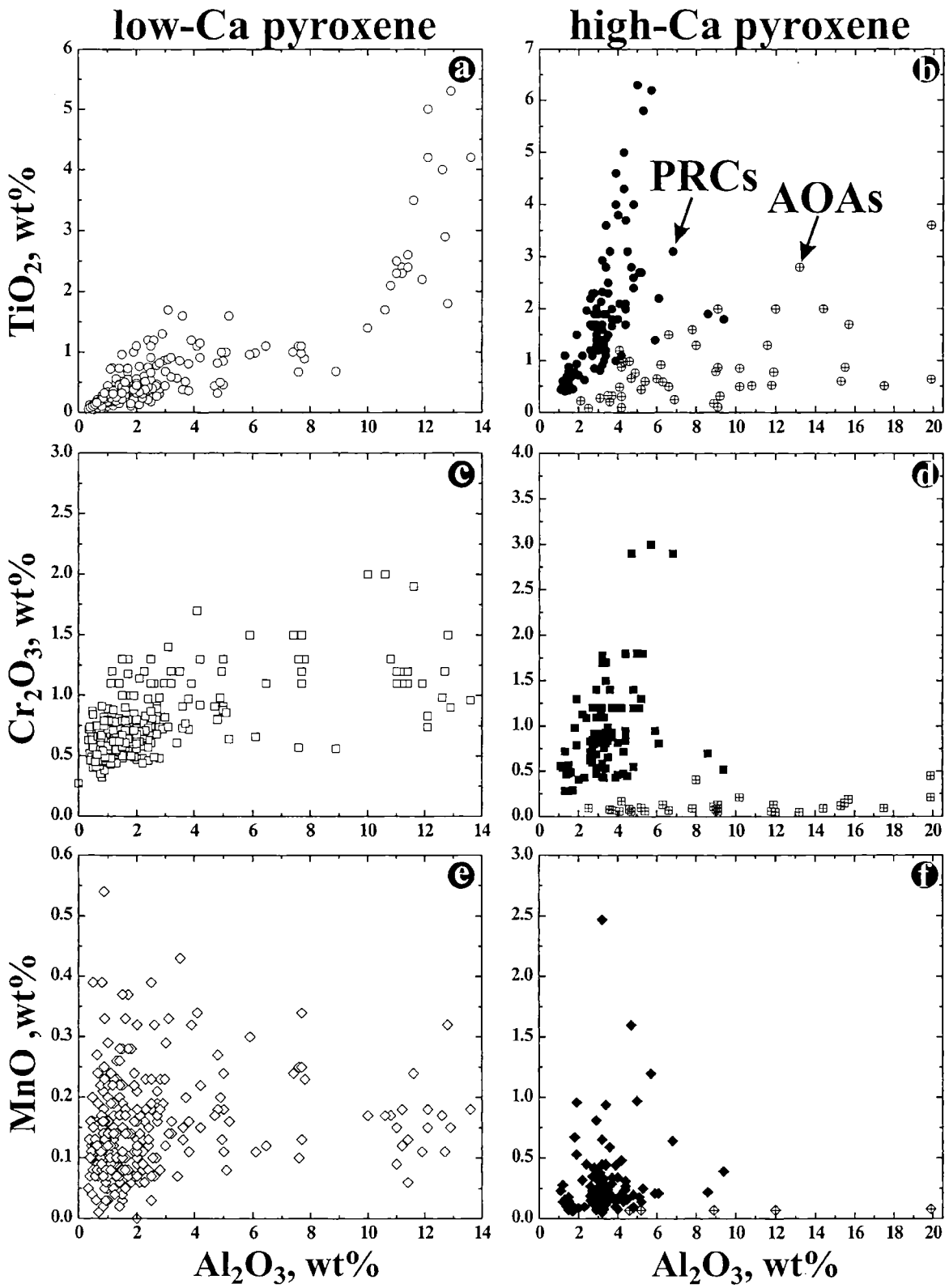

FIG. 4. Concentrations (in wt%) of TiO_2 (a, b), Cr_2O_3 (c, d) and MnO (e, f) *vs.* Al_2O_3 in low-Ca pyroxenes (a, c, e) and high-Ca pyroxenes (b, d, f) in the PRCs (empty and filled symbols) and AOAs (crossed symbols) in the reduced CV chondrites. Data for pyroxenes in AOAs are from Komatsu *et al.* (2001). High-Ca pyroxenes in the AOAs are enriched in Al_2O_3 and depleted in TiO_2, Cr_2O_3 and MnO compared to those in PRCs; low-Ca pyroxene has not been observed in the CV AOAs.

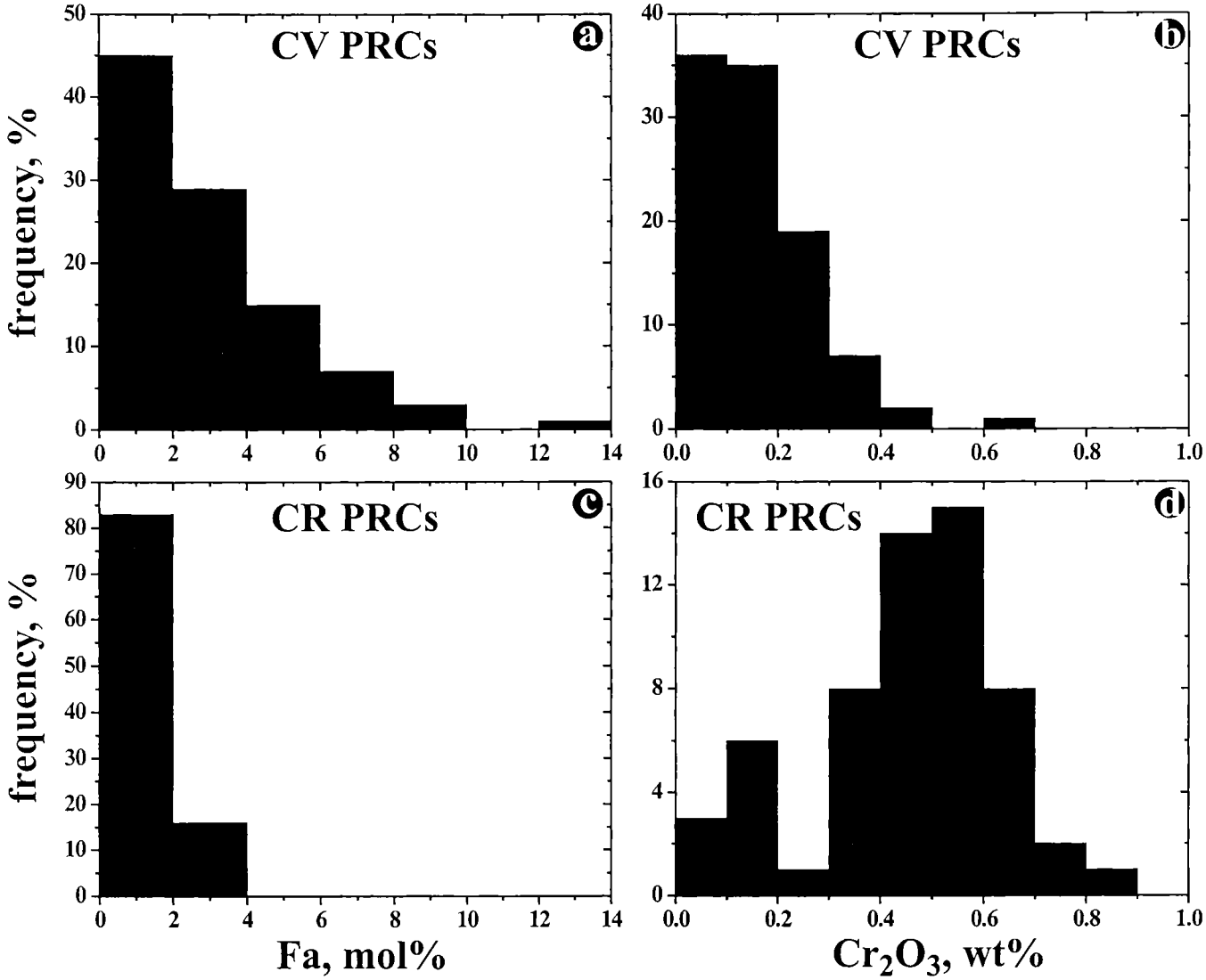

FIG. 5. Histograms of fayalite (Fa, mol%) and Cr_2O_3 (wt%) contents in olivine in PRCs in the reduced CV (a, b) and CR (c, d) chondrites. Data for olivine in the PRCs in CR chondrites are from Krot and Keil (2002).

TABLE 2. Representative microprobe analyses of low-Ca pyroxenes in PRCs in the reduced CV chondrites.

ox.\analysis	1	2	3	4	5	6
SiO_2	55.7	54.5	58.6	50.7	48.6	56.9
TiO_2	1.5	0.97	0.19	2.4	4.5	0.65
Al_2O_3	3.9	6.2	1.1	11.4	12.6	2.9
Cr_2O_3	0.70	1.3	0.59	1.2	0.88	0.70
FeO	0.74	0.79	0.67	0.67	1.1	1.3
MnO	0.16	0.25	0.09	0.13	0.17	0.11
MgO	36.4	34.8	38.3	32.8	31.6	36.6
CaO	1.7	1.0	0.43	0.57	0.51	1.3
Na_2O	<0.06	<0.06	<0.06	<0.06	<0.06	<0.06
K_2O	<0.04	<0.04	<0.04	<0.04	<0.04	<0.04
Total	100.7	99.9	99.9	99.8	100.0	100.5
Fs	1.1	1.2	1.0	1.1	1.8	1.9
Wo	3.2	2.0	0.8	1.2	1.1	2.4

Analyses: 1 = PRC #1, GRO 93429 (8); 2–4 = PRC #2, Vigarano (UH 35); 5, 6 = PRC #2, Leoville (1).

TABLE 3. Representative microprobe analyses of high-Ca pyroxenes in PRCs in the reduced CV chondrites.

ox.\analysis	1	2	3	4	5	6
SiO_2	50.6	53.6	53.2	52.6	50.8	51.0
TiO_2	4.6	1.5	2.3	2.1	4.0	4.3
Al_2O_3	3.9	2.9	2.7	3.1	4.8	4.3
Cr_2O_3	0.43	0.69	0.85	1.2	0.55	0.48
FeO	0.43	0.98	0.72	0.64	0.83	0.45
MnO	0.14	0.22	0.18	0.27	0.10	0.14
MgO	18.6	21.3	21.1	19.61	20.2	18.0
CaO	21.0	19.5	19.4	20.72	19.2	21.7
Na_2O	<0.06	<0.06	<0.06	<0.06	<0.06	<0.06
K_2O	<0.04	<0.04	<0.04	<0.04	<0.04	<0.04
Total	99.7	100.8	100.4	100.4	100.4	100.5
Fs	0.7	1.5	1.1	1.0	1.4	0.8
Wo	44.5	39.1	39.4	42.7	40.1	46.1

Analyses: 1 = PRC #1, GRO 93429 (8); 2 = PRC #2, Efremovka (2); 3 = PRC #1, Leoville (4); 4 = PRC #22, Efremovka (3-7-22); 5, 6 = PRC #14, Efremovka (8-7-22).

TABLE 4. Representative microprobe analyses of olivine in PRCs in the reduced CV chondrites.

ox.\analysis	1	2	3	4	5	6	7	8	9	10	11	12
SiO_2	42.1	42.5	41.8	42.3	41.9	41.0	42.3	42.0	42.4	42.1	41.4	42.1
TiO_2	0.05	0.30	0.07	0.08	0.05	<0.04	0.06	0.06	0.08	0.06	0.06	<0.04
Al_2O_3	0.03	0.27	0.05	0.04	0.04	0.04	0.07	0.16	0.09	0.11	0.16	0.04
Cr_2O_3	0.07	0.13	<0.06	0.11	0.13	0.06	0.12	0.16	0.20	0.25	0.22	0.15
FeO	4.0	0.81	3.2	2.1	2.4	7.2	1.1	1.5	1.5	1.3	3.8	2.6
MnO	0.12	<0.07	0.07	<0.07	0.13	0.15	0.11	<0.07	0.12	0.14	<0.07	0.15
MgO	54.9	57.0	55.4	56.0	54.7	50.9	55.8	56.2	56.2	55.9	53.6	54.6
CaO	0.16	0.21	0.15	0.18	0.15	0.10	0.10	0.58	0.14	0.30	0.30	0.20
Total	101.4	101.3	100.7	100.9	99.6	99.5	99.7	100.7	100.7	100.2	99.6	99.9
Fa	3.9	0.8	3.1	2.0	2.4	7.4	1.1	1.4	1.4	1.3	3.9	2.6

Analyses: 1, 2 = PRC #14, Efremovka (8-7-22); 3, 4 = PRC #1, GRO 93429 (8); 5–7 = PRC #2, Vigarano (UH 35); 8, 9 = PRC #1, Leoville (4); 10–12 = PRC #22, Efremovka (3-7-22); 10 = host. chondrule; 11 = POP #1; 12 = POP #2.

TABLE 5. Representative microprobe analyses of plagioclase in PRCs in the reduced CV chondrites.

ox.\analysis	1	2	3	4	5	6	7
SiO_2	46.0	44.2	46.0	44.9	44.2	46.0	45.6
TiO_2	0.10	0.08	0.05	0.06	0.04	0.04	0.05
Al_2O_3	33.4	35.5	33.9	34.4	34.5	33.4	33.7
Cr_2O_3	<0.06	<0.06	<0.06	<0.06	<0.06	<0.06	0.08
FeO	1.3	0.32	0.41	0.33	0.31	0.70	0.62
MnO	<0.07	<0.07	<0.07	<0.07	<0.07	<0.07	<0.07
MgO	0.39	0.31	0.23	0.50	0.41	0.65	0.58
CaO	17.5	19.1	17.4	18.4	18.3	17.9	17.7
Na_2O	1.6	0.70	1.9	1.2	1.3	1.5	1.3
K_2O	<0.04	<0.04	<0.04	<0.04	<0.04	<0.04	<0.04
Total	100.4	100.3	100.0	99.9	99.1	100.3	99.7
Ab	14.2	6.2	16.6	10.7	11.1	13.3	11.4
An	85.8	93.7	83.4	89.2	88.9	86.7	88.6

Analyses: 1, 2 = PRC #14, Efremovka (8-7-22); 3, 4 = PRC #2 Vigarano (UH 35); 5 = PRC #1, GRO 93429 (8); 6, 7 = PRC #1, Leoville (4).

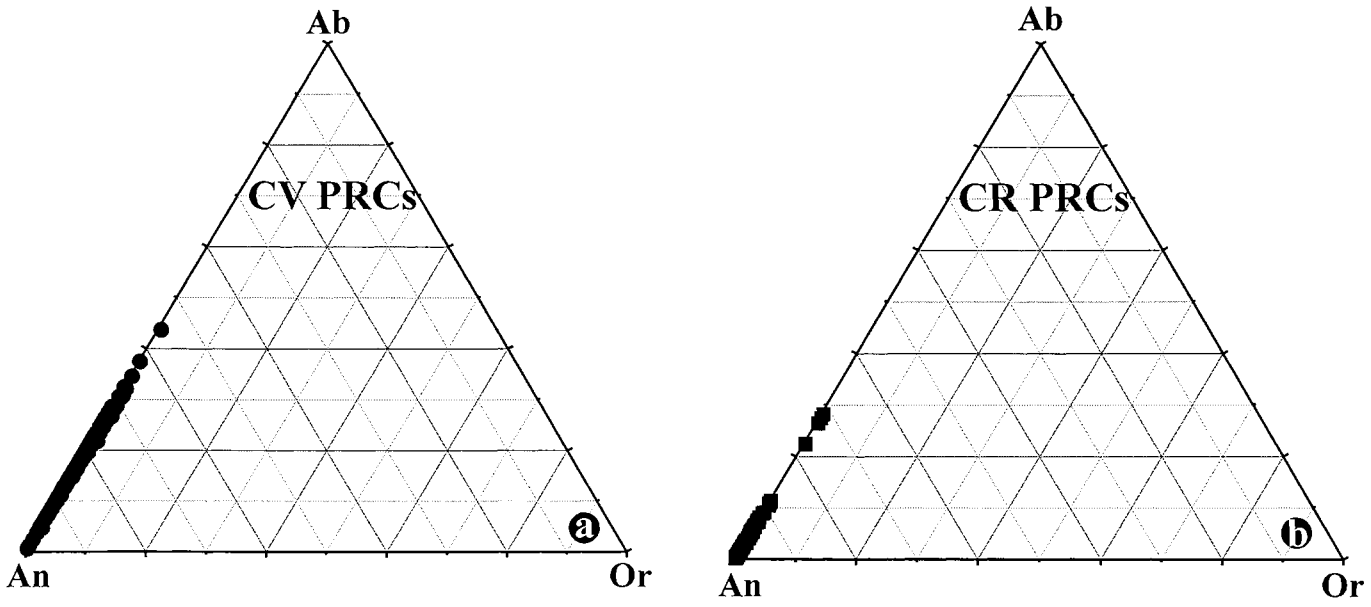

FIG. 6. Compositions of plagioclase in PRCs in the reduced CV (a) and CR (b) chondrites. Data for plagioclase in the PRCs in CR chondrites are from Krot and Keil (2002).

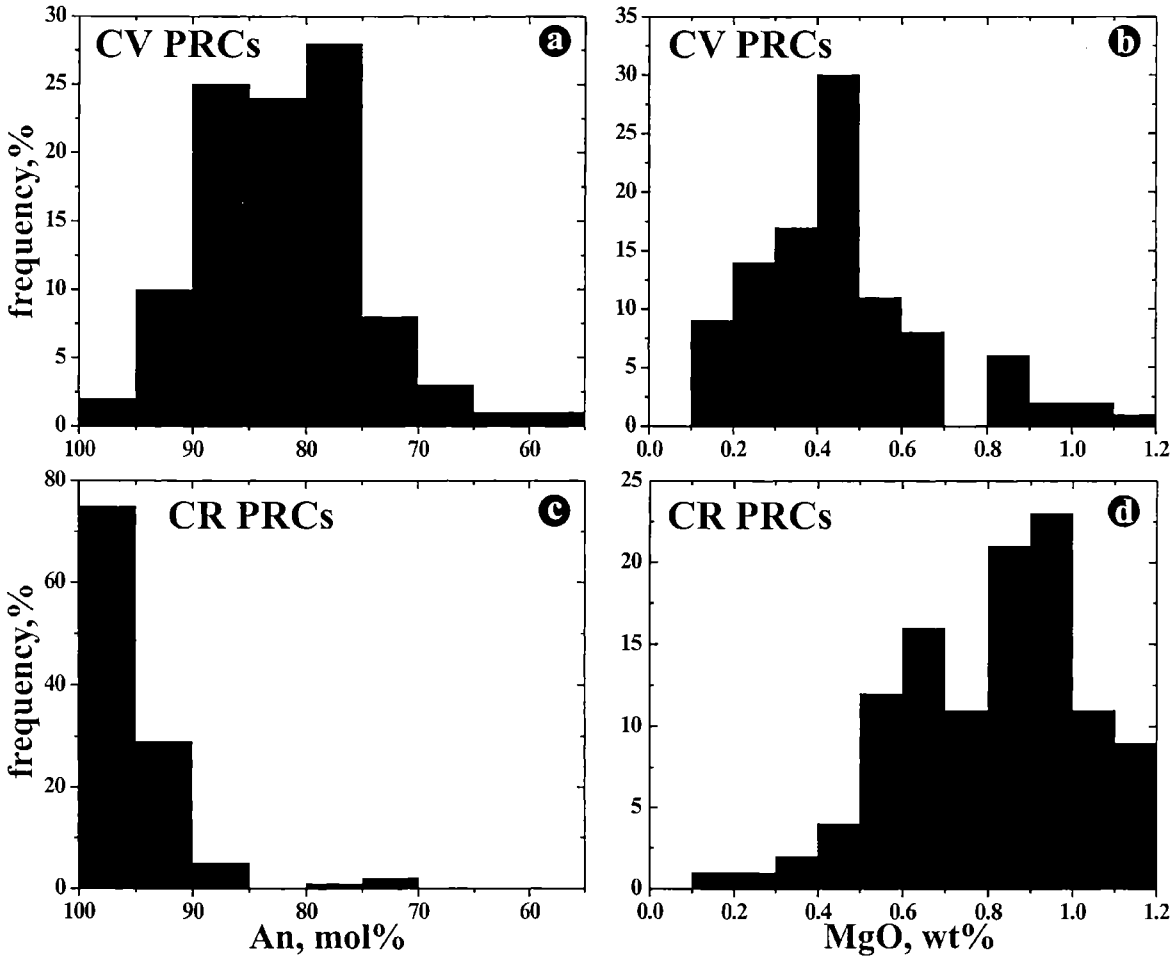

FIG. 7. Histograms of anorthite (An, mol%) and MgO contents (wt%) in plagioclase in PRCs in the reduced CV (a, b) and CR (c, d) chondrites. Data for plagioclase in the PRCs in CR chondrites are from Krot and Keil (2002).

TABLE 6. Microprobe analyses of spinel in PRCs in the reduced CV chondrites.

ox.\analysis	1	2	3	4	5	6	7	8	9	10
SiO_2	0.09	0.17	0.10	0.17	0.15	0.15	0.09	0.07	0.10	0.47
TiO_2	0.42	0.30	0.55	0.38	0.91	0.54	0.59	1.9	1.4	0.65
Al_2O_3	69.5	70.2	70.6	69.4	66.2	67.2	69.5	69.3	69.0	69.1
Cr_2O_3	1.6	0.70	0.28	1.2	5.0	3.1	0.74	1.3	0.95	1.1
FeO	1.7	2.0	0.67	0.64	2.3	4.8	3.2	1.0	5.1	0.47
MnO	<0.07	<0.07	<0.07	0.08	0.07	<0.07	<0.07	<0.07	<0.07	0.07
MgO	27.0	27.7	27.8	27.9	25.8	24.7	26.1	27.0	25.0	27.8
CaO	0.08	<0.04	0.04	0.07	0.04	<0.04	0.06	0.07	0.05	0.29
V_2O_3	0.21	0.16	n.a.	0.61	n.a.	n.a.	0.13	n.a.	n.a.	0.77
Total	100.4	100.1	100.1	99.9	100.5	100.6	100.3	100.7	101.7	100.1
fe	3.4	4.0	1.3	1.3	4.7	9.8	6.4	2.1	10.3	0.9

Analyses: 1, 2 = PRC #1, Leoville (4); 3, 4 = PRC #2, Leoville (1); 5, 6 = PRC #2, Vigarano (UH 35); 7 = PRC #1, GRO 93429 (8);

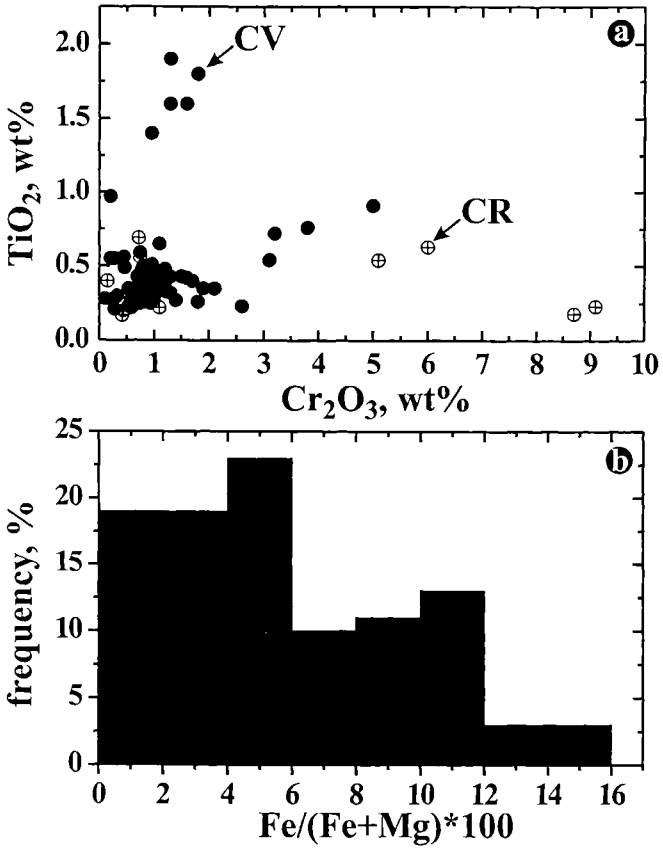

FIG. 8. Concentrations of Cr_2O_3 *vs.* TiO_2 and histograms of Fe/(Fe + Mg) × 100 ratios of spinel (only in the reduced CV) in PRCs in the the reduced CV (filled circles) and CR (crossed circles) chondrites.

Inclusions Associated with Plagioclase-Rich Chondrules"). Olivine grains are forsterite-rich ($Fa_{<14}$, with a peak at ~Fa_{0-4}) and Cr-poor (Table 4; Fig. 5a,b). Plagioclase grains are K-free and Ca-rich (An_{55-100}, with a peak at An_{75-90}); all plagioclase analyses show detectable MgO (0.1–1.2 wt%)

TABLE 7. Microprobe analyses of secondary minerals in PRCs in Vigarano.

ox.\analysis min.	1 nph	2 hd	3 fa
SiO_2	42.9	31.9	34.2
TiO_2	<0.04	<0.04	0.21
Al_2O_3	35.0	<0.03	1.2
Cr_2O_3	<0.06	<0.06	0.63
FeO	0.09	34.4	37.6
MnO	<0.07	0.23	0.32
MgO	0.24	1.9	23.9
CaO	0.12	30.0	0.4
Na_2O	21.5	<0.06	<0.06
K_2O	<0.04	<0.04	<0.04
Total	99.8	98.4	98.5
Fa	–	–	47.0
Fs	–	45.1	–
Wo	–	50.5	–

Analyses: 1 = PRC #2, Vigarano (UH 35); 2 = PRC #1, Vigarano (UH 63); 3 = PRC #3, Vigarano (UH 35).
Abbreviations: nph = nepheline, hd = hedenberge, fa = fayalitic olivine.

(Table 5; Figs. 6a and 7a,b). Spinel grains are magnesium-rich (Fe/(Fe + Mg) < 0.16) and contain relatively high TiO_2 (up to 2 wt%) and Cr_2O_3 (up to 5 wt%) (Table 6; Fig. 8).

Secondary nepheline replacing anorthitic plagioclase (Fig. 1c,d) is Ca-poor and K-free (Table 7). Secondary pyroxenes replacing silica in chondrule mesostases have ferrosilite-hedenbergite compositions (Table 7). Secondary olivine (~Fa_{50}) replaces low-Ca pyroxene, forms rims around forsterite grains and is present as haloes around FeNi-metal inclusions in forsterite; all these textural occurrences of secondary olivine have been previously described in detail by Hua *et al.* (1988) and are not illustrated here.

Igneous Rims Around Plagioclase-Rich Chondrules

About 50% of all type I chondrules in CV chondrites are surrounded by coarse-grained igneous rims (Rubin and Krot, 1996). Only a few PRCs, however, were found to be surrounded by such rims (Figs. 2c,d, and 9).

The coarse-grained igneous rim around PRC #2 in Efremovka (E 105) (Fig. 2d,e) is texturally and mineralogically similar to those around ferromagnesian chondrules in type 3 ordinary and carbonaceous chondrites (Rubin, 1984; Krot and Wasson, 1995). It has a porphyritic texture and consists of forsteritic olivine, low-Ca pyroxene, opaque nodules and mesostasis; low-Ca pyroxene is largely concentrated in the peripheral portion of the rim. The fayalite and ferrosalite contents of olivine (Fa_{1-3}) and pyroxene (Fs_{1-3}) in the host chondrule and igneous rim are similar.

The igneous rim around PRC #22 in Efremovka (3-7-2) is fine-grained and consists of microphenocrysts of low-Ca pyroxene embedded in a very fine-grained Ca-rich material, composed of Al-rich pigeonite and auigite, anorthitic plagioclase, and abundant opaque nodules (Fig. 9). This rim surrounds not only the host PRC, but also two POP chondrules and a radial pyroxene (RP) chondrule; these chondrules are also magnesium-rich (analyses 10–12 in Table 4). This complex object is surrounded by a fine-grained matrix-like rim largely composed of ferrous olivine (~Fa_{50}).

Compound Plagioclase-Rich Chondrules

Two of the PRCs in Leoville form compound objects (Fig. 10). Although in both cases the chondrules forming compound objects are anorthite-rich, they are texturally and mineralogically different from each other and can be classified as independent (Wasson *et al.*, 1994).

The upper PRC of the compound chondrule #2 in Leoville (1) has an Al-rich core composed of coarse lath-shaped anorthitic plagioclase (An_{91}) with abundant inclusions of Cr-bearing spinel (analyses 3 and 4 in Table 6), anhedral grains of forsteritic olivine (Fa_1) and Al-Ti-rich low-Ca pyroxene (in wt%, TiO_2, 4.5; Al_2O_3, 12.6; Cr_2O_3, 0.9; analysis 5 in Table 2) (Fig. 10a–c). This Al-rich core may have resulted from crystallization of melt produced by remelting of CAI (see section "Refractory Inclusions Associated with Plagioclase-Rich Chondrules"). The outer portion of the chondrule consists of fine-grained anorthitic plagioclase (An_{91}) and pigeonite-augite pyroxenes; it also contains several coarse grains of forsteritic olivine (Fa_3). The plagioclase grains near the chondrule periphery are replaced by nepheline. The lower PRC is mineralogically similar to the outer portion of the upper PRC; it consists of forsteritic olivine (Fa_4) and low-Ca pyroxene (in wt%, TiO_2, 0.7; Al_2O_3, 2.9; Cr_2O_3, 0.7; analysis 6 in Table 2) phenocrysts containing abundant inclusions of opaque nodules, anorthitic plagioclase (An_{91}), and pigeonite-augite pyroxenes.

The upper PRC of the compound chondrule #1 in Leoville (4) has a microporphyritic texture and consists of forsteritic olivine (Fa_{1-4}; analysis 8 in Table 4), low-Ca pyroxene (in wt%, TiO_2, 0.9; Al_2O_3, 3.0; Cr_2O_3, 1.1) and anorthitic plagioclase (An_{86}). It also contains an irregularly-shaped Al-rich region composed of Cr-bearing spinel (analysis 1 in Table 6), anorthitic plagioclase (An_{94}), Al-Ti-Cr-rich low-Ca pyroxene (in wt%, TiO_2, 2.2; Al_2O_3, 10.7; Cr_2O_3, 1.9) and nearly pure forsterite ($Fa_{0.2}$) (Fig. 10d–f). This Al-rich core may have resulted from crystallization of melt produced by remelting of CAI (see section "Refractory Inclusions Associated with Anorthite-Rich Chondrules"). The lower PRC has a porphyritic texture and consists of coarse-grained forsterite (Fa_{1-4}; analysis 9 in Table 4), low-Ca pyroxene (in wt%, TiO_2, 0.2; Al_2O_3, 0.7; Cr_2O_3, 0.5), anorthitic plagioclase (An_{86}), interstitial pigeonite, augite and silica-rich crystalline mesostasis; several Cr-bearing spinel grains (analysis 2 in Table 6) occur as inclusions in one of the forsterite grains.

Refractory Inclusions Associated with Plagioclase-Rich Chondrules

Twelve PRCs (including two compound PRCs described above) contain refractory inclusions that are mineralogically distinct from the host chondrules and may represent relic CAIs partly melted during chondrule formation (see "Relic Origin of Calcium-Aluminum-Rich Inclusions in Plagioclase-Rich Chondrules"); six of these objects (three irregularly-shaped and three rounded) are described below.

Plagioclase-rich chondrule #21 in Leoville (UH 122) is an irregularly-shaped object that has a microporphyritic olivine texture and consists of forsterite (Fa_2), low-Ca pyroxene (Fs_2Wo_7; in wt%, TiO_2, 0.6; Al_2O_3, 1.7; Cr_2O_3, 0.3), abundant FeNi-metal nodules, lath-shaped anorthitic plagioclase (An_{87}), and minor high-Ca pyroxene (Fs_2Wo_{38}; in wt%, TiO_2, 1.7; Al_2O_3, 5.0; Cr_2O_3, 0.2) (Fig. 11). The low-Ca pyroxene grains are largely concentrated in the chondrule periphery and poikilitically enclose forsterite. An irregularly-shaped Ca,Al-rich refractory inclusion intergrown with the PRC lacks opaque nodules and olivine and consists of fine-grained anorthitic plagioclase (An_{98}), anhedral high-Ca and low-Ca pyroxenes and tiny grains of secondary nepheline; the pyroxenes are too fine-grained for microprobe analysis.

Plagioclase-rich chondrule #66 in Leoville (UH 122) is an irregularly-shaped object that has a microporphyritic texture and consists of forsterite (Fa_{2-4}), low-Ca pyroxene (Fs_2Wo_3; in wt%, TiO_2, 0.6; Al_2O_3, 3.2; Cr_2O_3, 0.6), abundant FeNi-metal nodules, anorthitic plagioclase (An_{92}), and high-Ca pyroxene (Fs_2Wo_{38}; in wt%, TiO_2, 1.6; Al_2O_3, 3.8; Cr_2O_3, 0.5) (Fig. 12). The low-Ca pyroxene grains are concentrated in the chondrule periphery and poikilitically enclose forsterite. The chondrule contains a metal-free irregularly-shaped Ca,Al-rich refractory inclusion that consists of fine-grained spinel, anorthitic plagioclase (An_{95}), pigeonite-augite pyroxenes and

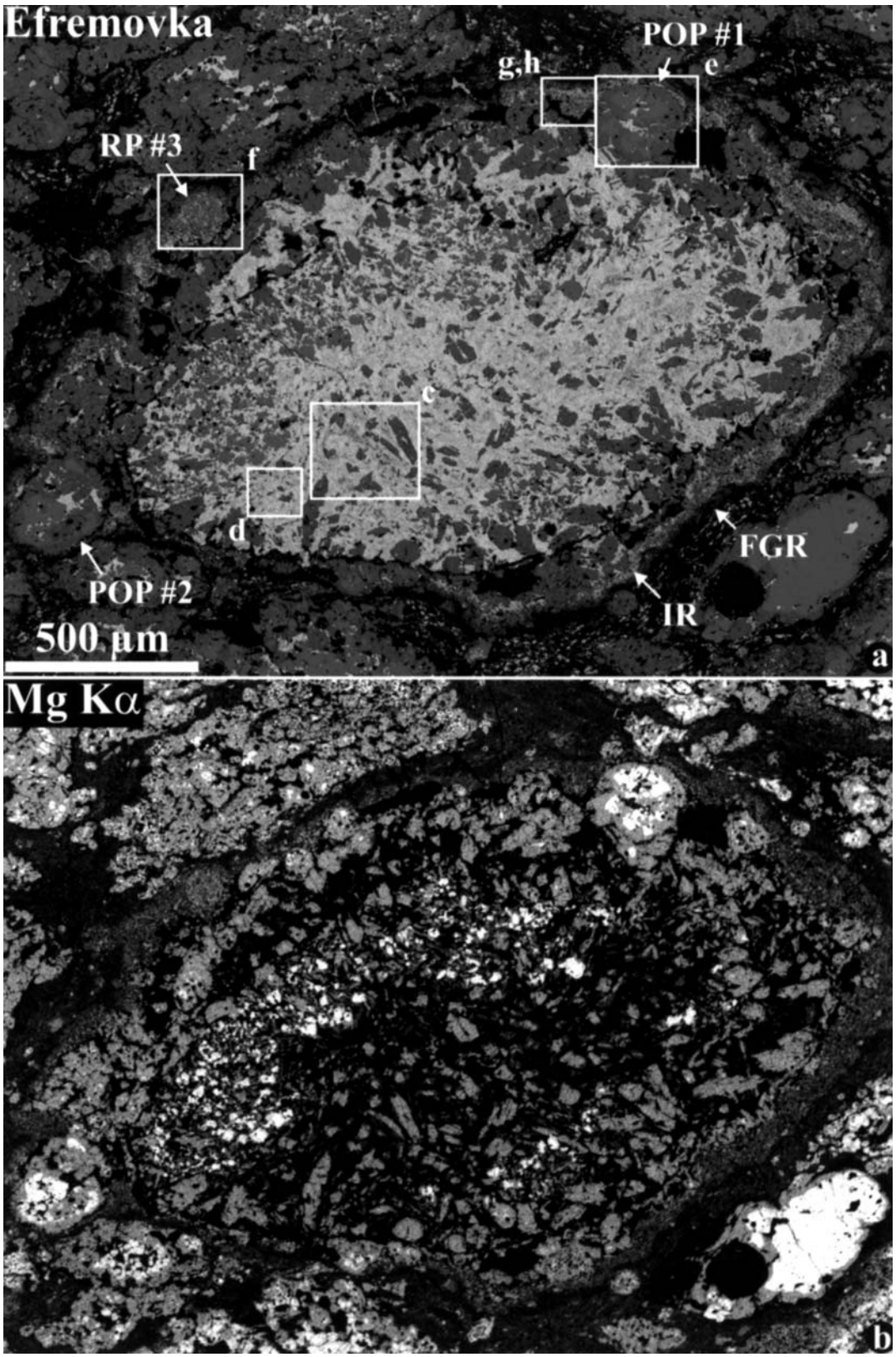

FIG. 9. Combined x-ray elemental map (a), elemental map in Mg Kα x-rays (b). Regions outlined and labeled in (a) are shown in detail in (c–h). (a–d) The chondrule consists of forsterite and low-Ca pyroxene phenocrysts, interstitial low-Ca and high-Ca pyroxenes, anorthitic plagioclase and fine-grained mesostasis composed of plagioclase, silica and high-Ca pyroxene. The plagioclase grains contain abundant inclusions of nepheline. The silica grains in mesostasis are largely replaced by Ca,Fe-rich pyroxene (bright white).

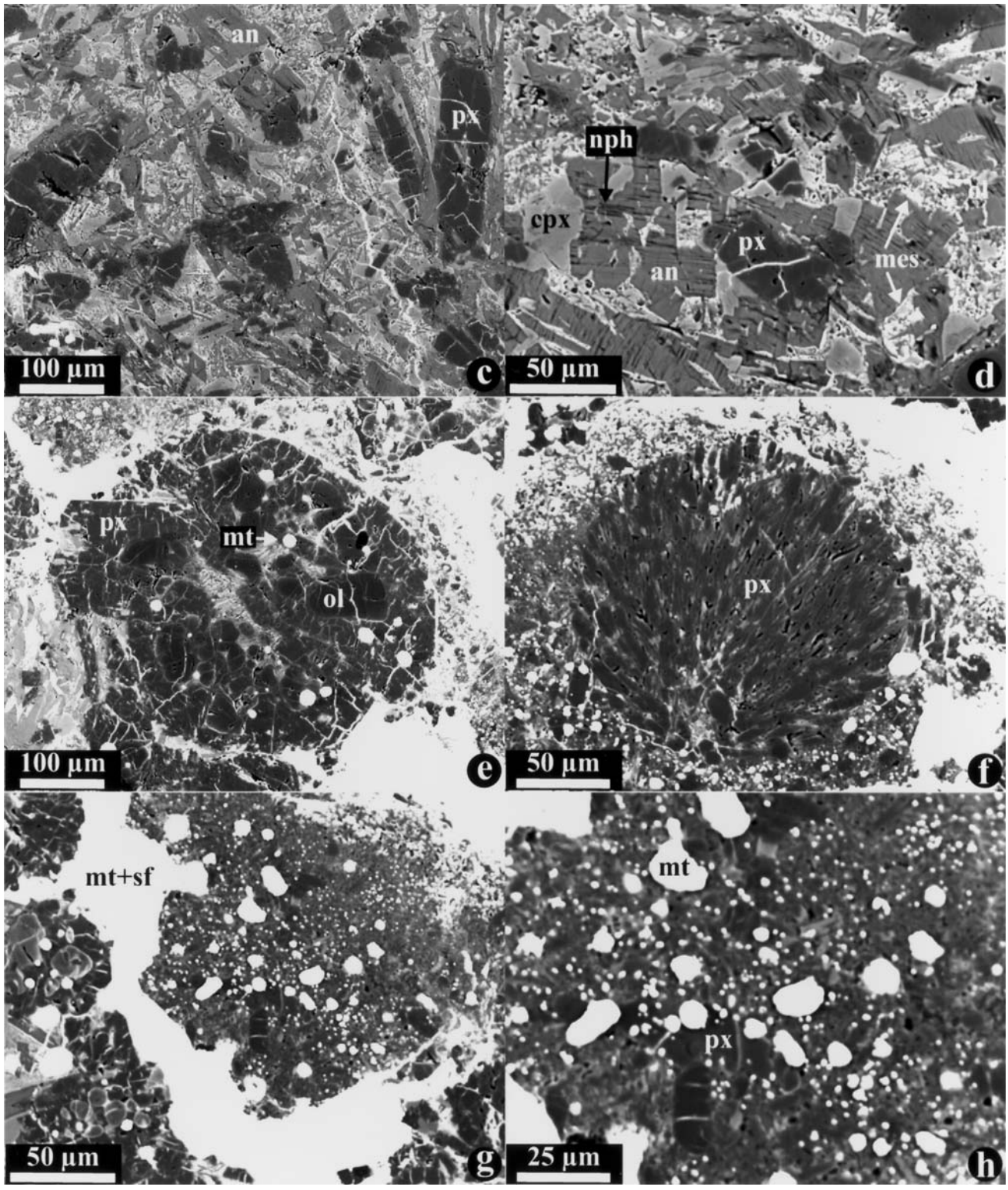

FIG. 9. *Continued.* Combined BSE images (c–h) of PRC #22 in Efremovka (3-7-2). Regions outlined and labeled in (a) are shown in detail in (c–h). (a–d) The chondrule consists of forsterite and low-Ca pyroxene phenocrysts, interstitial low-Ca and high-Ca pyroxenes, anorthitic plagioclase and fine-grained mesostasis composed of plagioclase, silica and high-Ca pyroxene. The plagioclase grains contain abundant inclusions of nepheline. The silica grains in mesostasis are largely replaced by Ca,Fe-rich pyroxene (bright white). The PRC, two porphyritic olivine-pyroxene chondrules (POP #1 (see (e)) and #2) and a radial pyroxene chondrule (RP #3, see (f)) are all surrounded by a fine-grained, metal-sulfide-rich igneous rim (IR, see (g) and (h)) and fine-grained matrix-like rim (FGR). The igneous rim contains small grains of low-Ca pyroxene and abundant opaque nodules embedded in a fine-grained material largely composed of high-Ca pyroxene and anorthite.

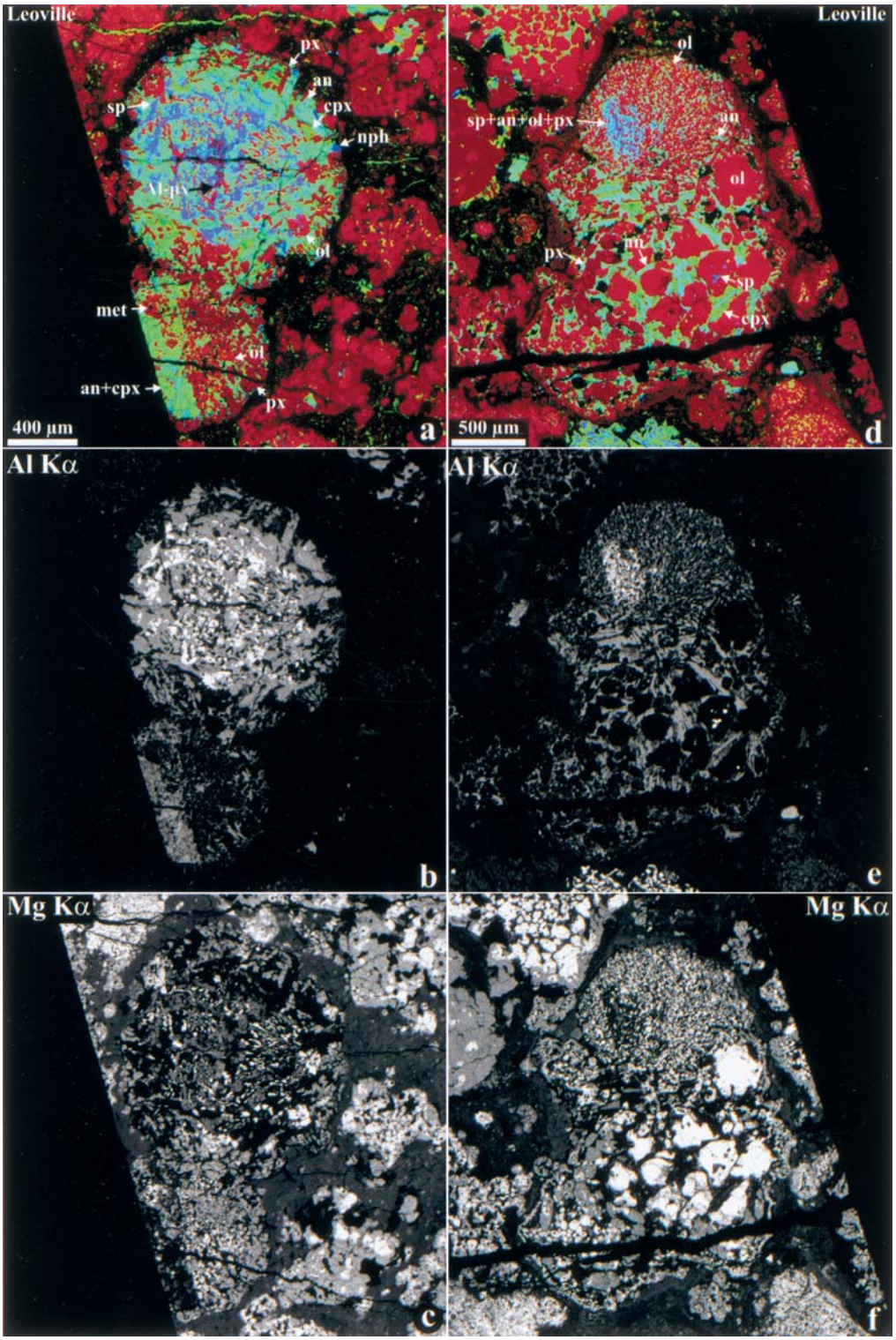

FIG. 10. Combined x-ray elemental maps in Mg (red), Ca (green) and Al Kα (blue) (a, d) and elemental maps in Al (b, e) and Mg Kα x-rays (c, f) of the compound PRCs #2 (a–c) in Leoville (1) and #1 (e–f) in Leville (4). (a–c) The lower and upper chondrules consist of the forsterite and low-Ca pyroxene phenocrysts, interstitial anorthitic plagioclase and high-Ca pyroxene, and mesostasis. Plagioclase is partly replaced by nepheline. The central portion of the upper chondrule contains spinel, elongated grains of forsterite and Al-rich low-Ca pyroxene (Al-px). (d–f) The upper chondrule has a microporphyritic texture and consists of forsterite, low-Ca pyroxene and interstitial anorthitic plagioclase; a triangular Al-rich region within the upper chondrule is composed of spinel, Al-rich low-Ca pyroxene, forsterite and anorthitic plagioclase. The lower chondrule has a porphyritic texture and consists of the forsterite and low-Ca pyroxene phenocrysts, interstitial anorthitic plagioclase and high-Ca pyroxene, and crystalline silica-plagioclase-high-Ca pyroxene mesostasis. One of the forsterite phenocrysts contains inclusions of anhedral spinel grains.

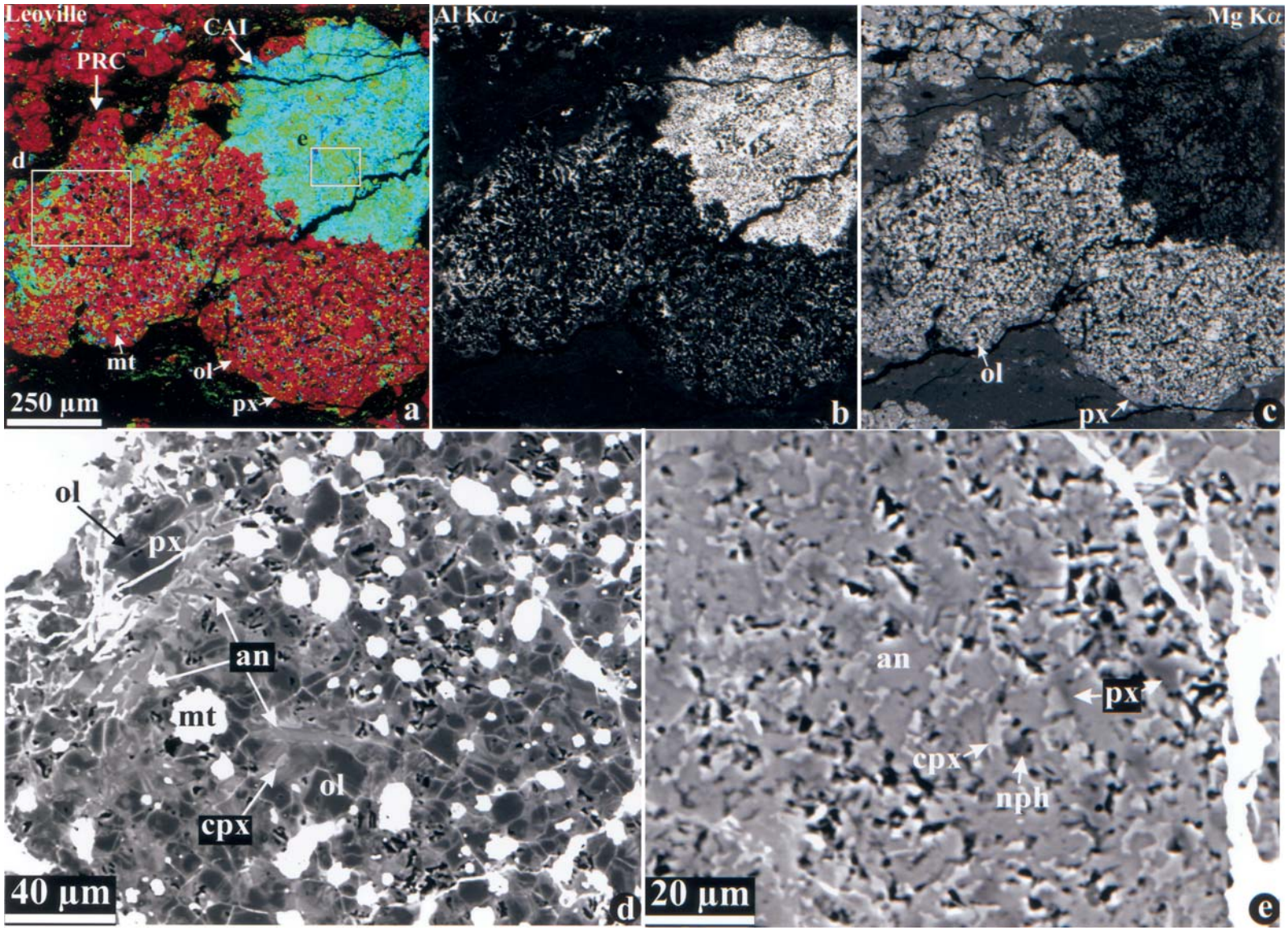

FIG. 11. Combined x-ray elemental map in Mg (red), Ca (green) and Al Kα (blue) (a), elemental maps in Al (b) and Mg Kα x-rays (c), and BSE images (d, e) of PRC #21 associated with CAI in Leoville (UH 122). Regions outlined and labeled in (a) are shown in detail in (d) and (e). The PRC consists of forsterite and low-Ca pyroxene phenocrysts, abundant FeNi-metal nodules and interstitial lath-shaped anorthitic plagioclase and high-Ca pyroxene. The low-Ca pyroxene grains are largely concentrated in the chondrule periphery. The CAI is metal-free and consists of fine-grained anorthite, anhedral high-Ca pyroxene and minor low-Ca pyroxene; secondary nepheline is very minor.

minor forsterite (Fa_{1-2}). The plagioclase grains of the refractory inclusion are partly replaced by nepheline; the plagioclase grains of the host chondrule are less altered (Fig. 12d).

Plagioclase-rich chondrule #14 in Efremovka (8-7-22) is an irregularly-shaped object that has a microporphyritic texture and consists of phenocrysts of forsteritic olivine (Fa_4; analysis 1 in Table 4) and low-Ca pyroxene (Fs_2Wo_5; in wt%, TiO_2, 0.9; Al_2O_3, 1.9; Cr_2O_3, 0.6), abundant FeNi-metal nodules, lath-shaped anorthitic plagioclase (An_{86}; analysis 1 in Table 5), elongated grains of pigeonite overgrown by augite (analyses 5 and 6 in Table 3) and fine-grained silica-bearing mesostasis (Fig. 13). The chondrule contains a large, metal-free irregularly-shaped Ca,Al-rich refractory inclusion. Fine-grained Cr-bearing spinel (analysis 8 in Table 6) intergrown with forsterite (Fa_1; analysis 2 in Table 4) forms core of the inclusion that is surrounded by anorthitic plagioclase (An_{94}; analysis 2 in Table 5) and pigeonite-augite pyroxenes. Plagioclase of the refractory inclusion is extensively replaced by nepheline (Fig. 13d,f); spinel grains in the altered regions of the inclusion are enriched in FeO (analysis 9 in Table 6). The plagioclase grains of the host chondrule are only slightly altered; chondrule mesostasis near the CAI, however, is more extensively replaced by secondary hedenbergitic pyroxene (Fig. 13d–f).

Plagioclase-rich chondrule #2 in Vigarano (UH 35) is a spherical object that has a porphyritic texture and consists of coarse forsterite grains (Fa_2; analysis 5 in Table 4), abundant opaque nodules, lath-shaped anorthitic plagioclase (An_{83}; analysis 4 in Table 5), elongated grains of Al-Ti-Cr-rich low-Ca pyroxene (Fs_1Wo_1, in wt%, TiO_2, 1.0; Al_2O_3, 6.2; Cr_2O_3, 1.3; analysis 2 in Table 2), augite and mesostasis (Fig. 14). The mesostasis is largely replaced by a fine-grained secondary Ca,Fe-rich material (in wt%, SiO_2, 51.7; TiO_2, 0.69; Al_2O_3, 10.1; Cr_2O_3, <0.06; FeO, 11.8; MnO, 0.12; MgO, 3.3; CaO, 19.7; Na_2O, 1.5; K_2O, <0.04; total, 99.1). The chondrule is surrounded by a shell of low-Ca pyroxene grains (Fs_1Wo_1, in wt%, TiO_2, 0.2; Al_2O_3, 1.1; Cr_2O_3, 0.6; analysis 3 in Table 2) containing abundant inclusions of forsteritic olivine (Fa_7; analysis 6 in Table 4) and opaque nodules (Fig. 14a,h). A rounded Ca,Al-rich refractory inclusion in the chondrule core consists of anorthitic plagioclase (An_{89}, analysis 4 in Table 5), Cr-bearing spinel (analyses 5 and 6 in Table 6), forsterite (Fa_1; analysis 7 in Table 4) and Al-Ti-Cr-rich low-Ca pyroxene (Fs_1Wo_1, in wt%, TiO_2, 2.4; Al_2O_3, 11.4; Cr_2O_3, 1.2) (Fig. 14a–g). The anorthitic plagioclase in the core of the inclusion contains thin sub-parallel inclusions of nepheline; plagioclase at the edge of the inclusion is extensively replaced by nepheline (Fig. 14b,f,g). A small region composed of the same secondary Ca,Fe-rich material as in the PRC was found in the core of the inclusion (Fig. 14d,e). Spinel grains in this region are enriched in FeO compared to those inside plagioclase, pyroxenes and forsterite (Fig. 14e).

Plagioclase-rich chondrule #1 in GRO 93429 (8) is a spherical object that has a porphyritic texture and consists of anorthitic plagioclase (An_{89}; analysis 5 in Table 5), anhedral grains of Al-Ti-Cr-rich low-Ca pyroxene (Fs_1Wo_3, in wt%, TiO_2, 1.5; Al_2O_3, 3.9; Cr_2O_3, 0.7; analysis 1 in Table 2) and type I chondrule-like regions composed of forsterite (Fa_3; analysis 3 in Table 4), low-Ca pyroxene and abundant FeNi-metal nodules (Fig. 15). The anorthitic plagioclase contains thin sub-parallel inclusions of nepheline; the abundance and size of the nepheline inclusions increase towards the chondrule periphery (Fig. 15b). The core of the chondrule contains an Ca,Al-rich region that is mineralogically similar to the Ca,Al-rich refractory inclusion in the PRC #2 in Vigarano (UH 35) described above. It consists of euhedral Cr-bearing spinel grains (analysis 7 in Table 6) and anhedral, elongated grains of forsterite (Fa_2; analysis 4 in Table 4), embedded in massive anorthitic plagioclase.

Plagioclase-rich chondrule #1 in Leoville (1) is an ellipsoidal object that has a porphyritic texture and consists of lath-shaped anorthitic plagioclase (An_{78}), elongated grains of pigeonite (Fs_1Wo_8, in wt%, TiO_2, 0.4; Al_2O_3, 1.4; Cr_2O_3, 0.8) overgrown by augite (Fs_1Wo_{38}, in wt%, TiO_2, 1.0; Al_2O_3, 2.6; Cr_2O_3, 0.7) and silica-plagioclase-augite mesostasis (Fig. 15). The upper portion of the chondrule contains a large concentration of coarse forsterite grains (Fa_2) surrounded by low-Ca pyroxene ($Fs_{1.6}Wo_{1.4}$, in wt%, TiO_2, 0.2; Al_2O_3, 0.6; Cr_2O_3, 0.4). The lower portion of the chondrule contains a rounded Al-rich object composed of anorthite (An_{98}) and containing rare inclusions of Cr-bearing spinel (analysis 10 in Table 6); the anorthite is extensively replaced by nepheline.

DISCUSSION

Genetic Links Between Plagioclase-Rich Chondrules, Plagioclase-Olivine Inclusions and Ferromagnesian Type I Chondrules in CV Chondrites

The plagioclase-rich chondrules in the reduced CV chondrites resemble plagioclase-olivine inclusions (POIs) described in the oxidized CV chondrite Allende (Sheng *et al.*, 1991). The POIs consist mainly of plagioclase and olivine and range in bulk compositions from type C CAIs to PO chondrules. In contrast to the CAIs, POIs are characterized by the absence of melilite, platinum group element nuggets and Wark–Lovering rims, the abundance of olivine, a distinctive pyroxene composition (TiO_2/Al_2O_3 ratio of ~1), and more sodic plagioclase (An_{85-95}) (Sheng *et al.*, 1991). Our petrographic observations and those reported by Sheng *et al.* (1991) suggest that POIs are a subset of PRCs. A similar conclusion was reached by Kring and Holmen (1988) and Kring and Boynton (1990), who described PRCs in the oxidized CV chondrites Allende, Ningqiang and Kaba and the CO chondrite Kainsaz. Although PRCs in carbonaceous chondrites are Al-rich (>10 wt% bulk Al_2O_3) as defined by Bischoff and Keil (1984) for chondrules in ordinary chondrites, the former are mineralogically distinct and can be considered as a subset of the Al-rich chondrules.

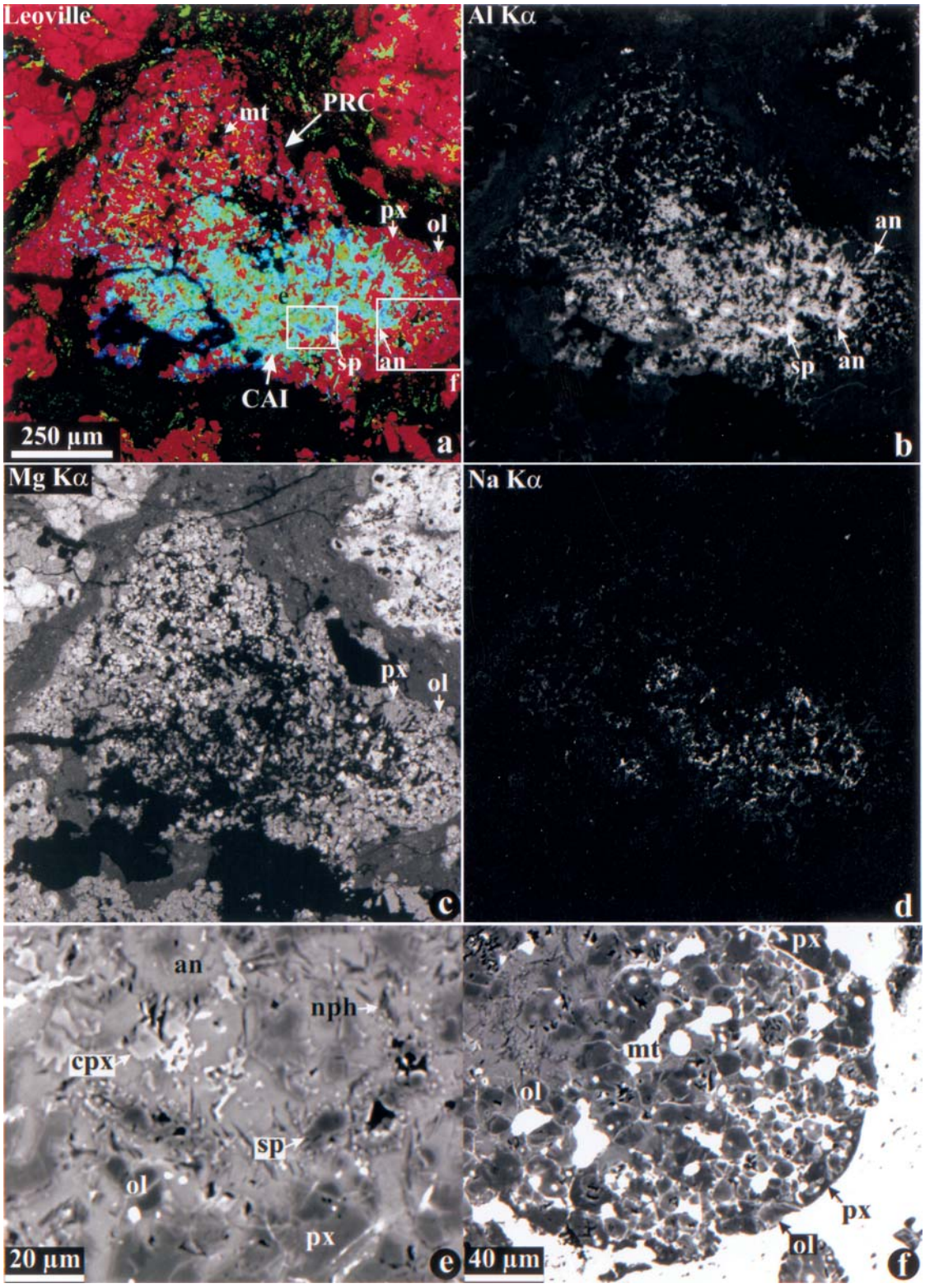

FIG. 12. Combined x-ray elemental map in Mg (red), Ca (green) and Al Kα (blue) (a), elemental maps in Al (b), Mg (c) and Na Kα x-rays (d), and BSE images (e, f) of PRC #66 with a relic CAI in Leoville (UH 122). Regions outlined and labeled in (a) are shown in detail in (e) and (f). The PRC consists of forsterite and low-Ca pyroxene phenocrysts, abundant FeNi-metal nodules and interstitial lath-shaped anorthitic plagioclase and high-Ca pyroxene. The low-Ca pyroxene grains poikilitically enclosing forsterite grains are largely concentrated in the chondrule periphery. The CAI is metal-free and consists of fine-grained spinel, anorthite, high-Ca pyroxene, and minor forsterite; anorthite is replaced by nepheline.

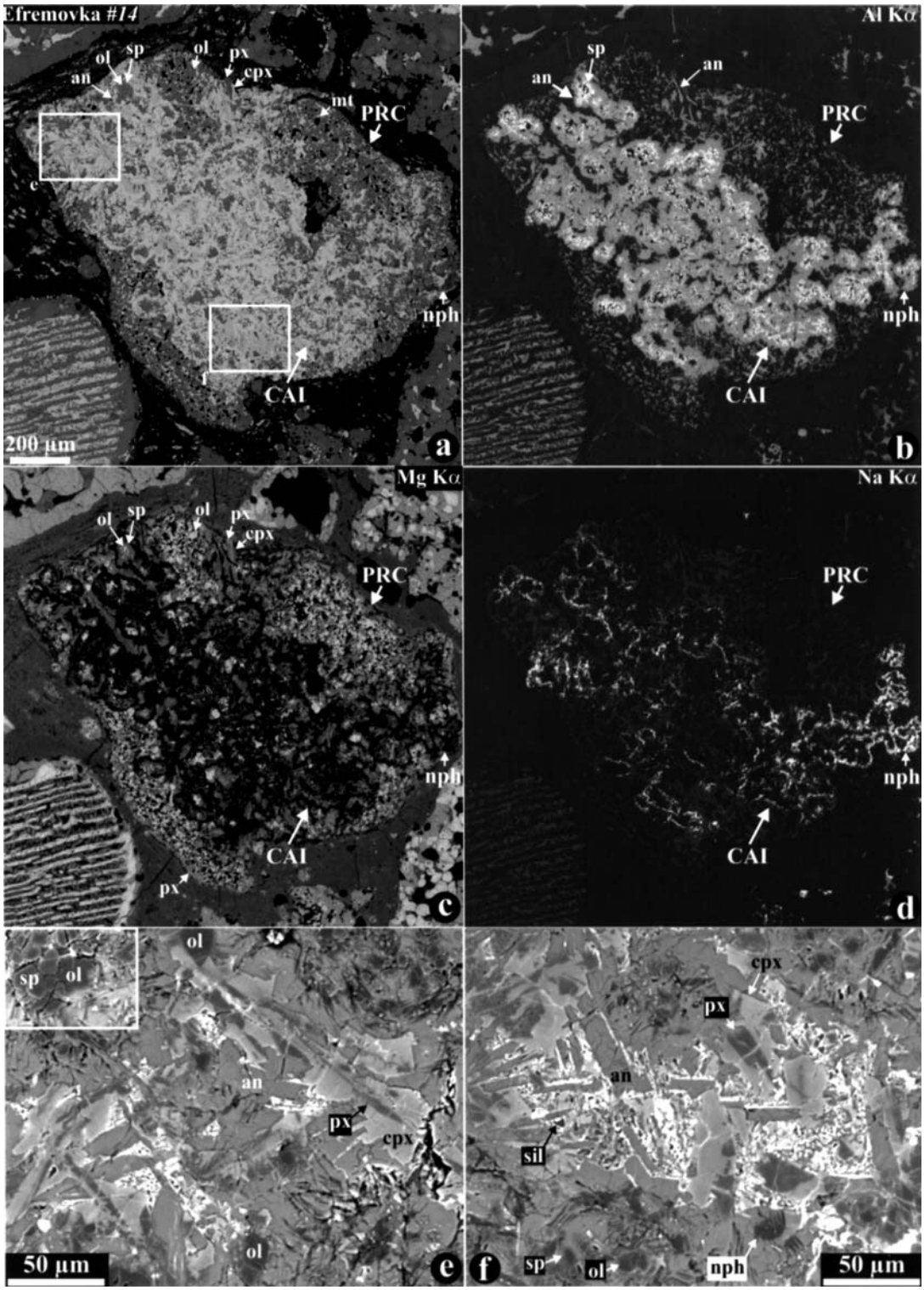

FIG. 13. Combined x-ray elemental map (a), elemental maps in Al (b), Mg (c) and Na Kα x-rays (d), and BSE images (e, f) of PRC #14 with a relic CAI in Efremovka (8-7-22). Regions outlined and labeled in (a) are shown in detail in (e) and (f); for the region outlined in (e) brightness and contrast were adjusted separately from the rest of the images. The PRC consists of forsterite and low-Ca pyroxene phenocrysts, interstitial elongated low-Ca pyroxene grains overgrown by high-Ca pyroxene, abundant FeNi-metal nodules, lath-shaped anorthitic plagioclase, and heavily-altered silica-bearing mesostasis; silica of the mesostasis is replaced by Ca,Fe-rich pyroxene (bright white). The CAI is metal-free and consists of fine-grained spinel intergrown with forsterite and surrounded by anorthite and high-Ca pyroxene; anorthite is extensively replaced by nepheline.

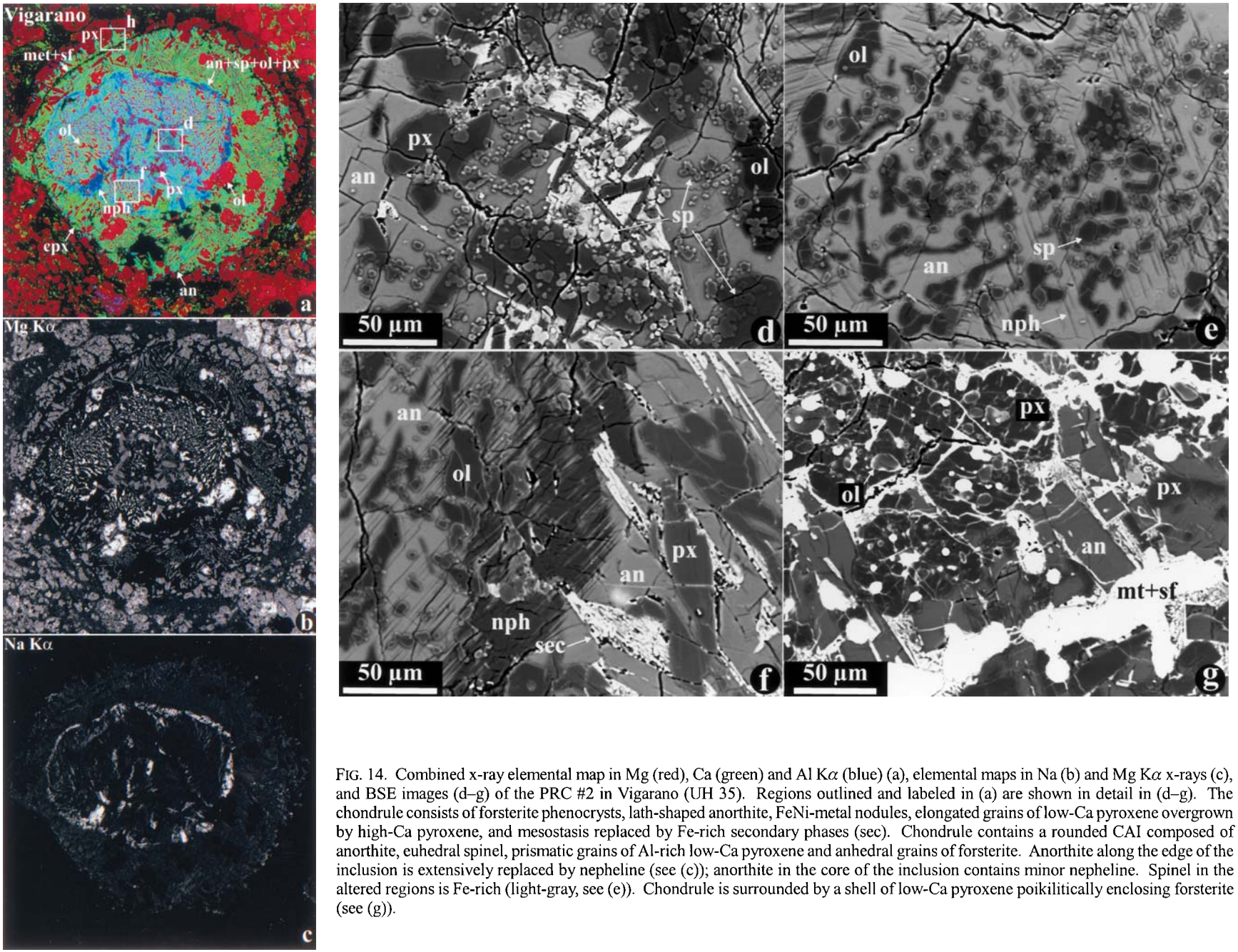

FIG. 14. Combined x-ray elemental map in Mg (red), Ca (green) and Al Kα (blue) (a), elemental maps in Na (b) and Mg Kα x-rays (c), and BSE images (d–g) of the PRC #2 in Vigarano (UH 35). Regions outlined and labeled in (a) are shown in detail in (d–g). The chondrule consists of forsterite phenocrysts, lath-shaped anorthite, FeNi-metal nodules, elongated grains of low-Ca pyroxene overgrown by high-Ca pyroxene, and mesostasis replaced by Fe-rich secondary phases (sec). Chondrule contains a rounded CAI composed of anorthite, euhedral spinel, prismatic grains of Al-rich low-Ca pyroxene and anhedral grains of forsterite. Anorthite along the edge of the inclusion is extensively replaced by nepheline (see (c)); anorthite in the core of the inclusion contains minor nepheline. Spinel in the altered regions is Fe-rich (light-gray, see (e)). Chondrule is surrounded by a shell of low-Ca pyroxene poikilitically enclosing forsterite (see (g)).

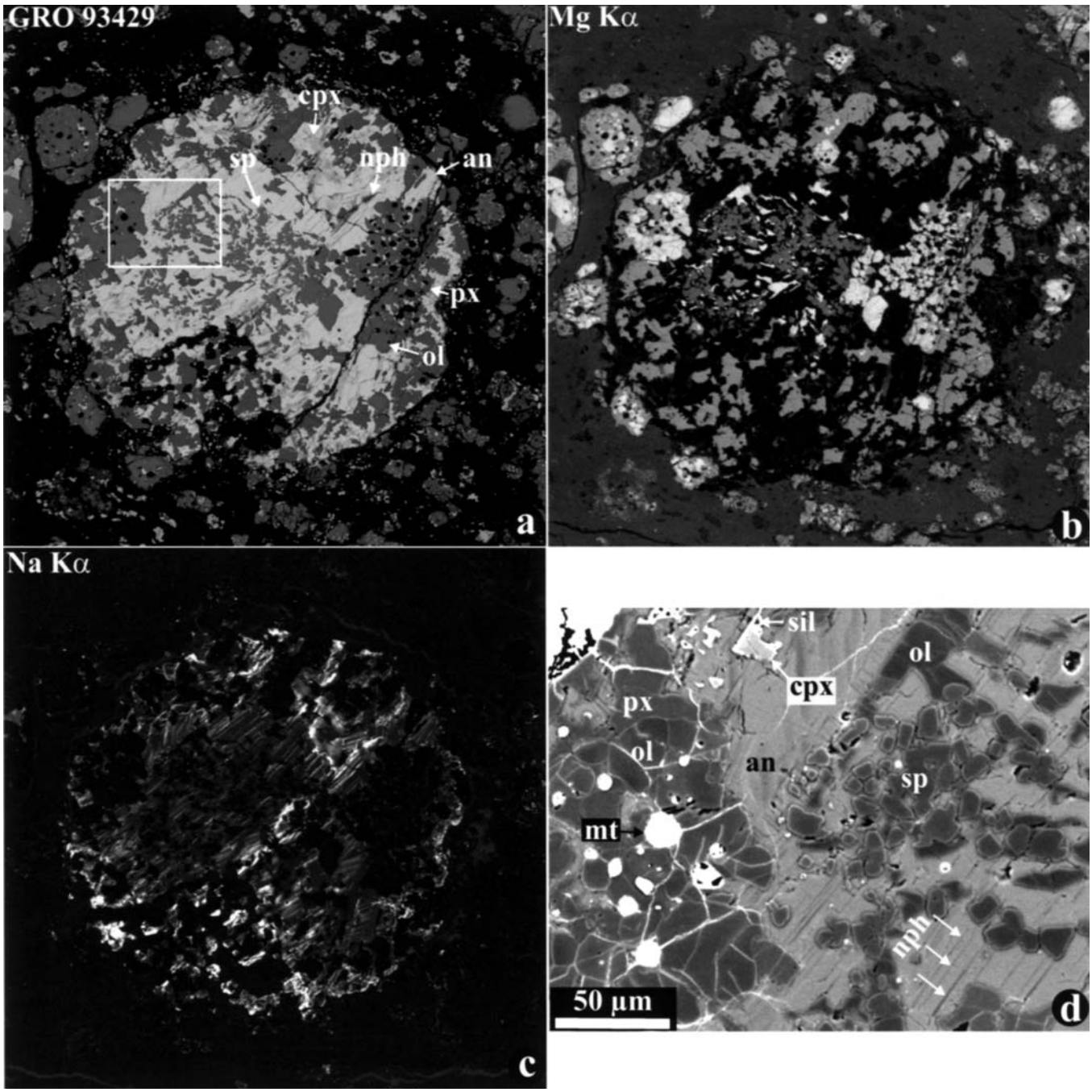

FIG. 15. Combined x-ray elemental map (a), elemental maps in Na (b) and Mg Kα x-rays (c), and BSE image (d) of the PRC #1 in GRO 93429 (8). Region outlined in (a) is shown in detail in (d). The chondrule consists of anorthite containing inclusions of euhedral spinel and anhedral forsterite, high-Ca pyroxene and minor silica-bearing mesostasis. It also contains regions composed of coarse-grained forsterite, low-Ca pyroxene and abundant FeNi-metal nodules. Anorthite grains are partly replaced by nepheline.

Sheng *et al.* (1991) excluded the possibility of formation of POIs as liquid or solid condensates from a solar gas or as evaporative residues and suggested that POIs formed by aggregation of isotopically dissimilar materials followed by partial melting. We suggest that PRCs are genetically related to ferromagnesian type I chondrules and formed as a result of melting of solid precursor materials in the chondrule-forming region(s), not in the CAI-forming region(s) (*e.g.*, Connolly and Love, 1998; Rubin, 2000; Jones *et al.*, 2000). The following petrographic observations support this conclusion. (1) Most of the PRCs have the typical droplet morphologies and igneous textures of chondrules and contain abundant FeNi-metal nodules

(Fig. 2). (2) Some of the PRCs are surrounded by igneous rims which are considered to be a result of repetitive chondrule-forming processes (Fig. 2c,d) (Krot and Wasson, 1995; Rubin and Krot, 1996). One of the igneous rims surrounds both the anorthite-rich and several magnesian type I chondrules, indicating that both chondrule types were present in the same region at the time of chondrule formation (Fig. 9). This conclusion is also supported by a compound chondrule composed of two ferromagnesian type I chondrules and an PRC found in Allende (Maruyama *et al.*, 1998a,b). (3) Many PRCs have continuous shells of low-Ca pyroxene around them (Figs. 2a,b, 11–13 and 14a,h); the similar shells are commonly observed around type I chondrules (*e.g.*, Jones and Scott, 1989), but are absent around CAIs. (4) Finally, several PRCs contain coarse-grained forsterite—low-Ca pyroxene—FeNi-metal regions that are texturally and mineralogically similar to type I chondrules (Figs. 15a and 16a). These regions appear to have been corroded by the host chondrule melts and may be relic in nature. In contrast to ferromagnesian chondrules, however, the PRC precursors commonly contained relic CAIs (see the following section).

Relic Origin of Calcium-Aluminum-Rich Inclusions in Plagioclase-Rich Chondrules

The presence of refractory grains in precursor materials for the Al-rich chondrules has previously been inferred from isotopic and trace element studies of a few Al-rich chondrules (*e.g.*, Misawa and Nakamura, 1988, 1996; Sheng *et al.*, 1991; Maruyama *et al.*, 1998a,b; Krot *et al.*, 1999; Hiyagon, 2000). The relic origin of the CAIs observed in several of the CV PRCs (Figs. 10–16) is inferred so far only from the mineralogical observations summarized below; trace element (volatility fractionated trace element patterns are expected for relic CAIs) and O-isotope studies (relic CAIs are expected to be ^{16}O-enriched relative to the host chondrules) are required to test this hypothesis.

The CAIs in the CV PRCs have different modal mineralogy than the host chondrules: (1) They lack FeNi-metal nodules, contain no or only very minor pigeonite-augite pyroxenes and higher abundance of anorthite and spinel. (2) They also have more anorthitic plagioclase than the host chondrules and contain a high abundance of spinel grains which occasionally form multiple cores of the objects (Figs. 12 and 13). Based on these observations, we infer that the CAIs and host PRCs did not crystallize from the same melt; the former are relic. We note, however, that most of the relic CAIs were probably melted to varying extents. The degrees of this melting appear to correlate with those of the host chondrules (*e.g.*, the irregularly-shaped PRCs contain irregularly-shaped CAIs having multiple spinel-rich cores) suggesting lack of appreciable melting (Figs. 12 and 13). The rounded CAIs occur inside rounded PRCs; the former lack multiple core structures and contain euhedral spinel grains intergrown with elongated forsterite and Al-rich low-Ca pyroxenes; these minerals appear to have crystallized from incompletely homogenized chondrule melts *in situ* (Figs. 10, 14 and 15).

Genetic Relationship of Plagioclase-Rich Chondrules and Amoeboid Olivine Aggregates in the Reduced CV Chondrites

It was recently suggested that Al-rich chondrules may have formed by melting of amoeboid olivine aggregates (AOAs) (A. Rubin, pers. comm.). There are some problems with this hypothesis. (1) Although the relic CAIs in the PRCs are mineralogically most similar to CAIs associated with AOAs in the reduced CV chondrites, which are mainly composed of anorthite, pyroxene and spinel (*e.g.*, Bar-Matthews *et al.*, 1979; Komatsu *et al.*, 2001), there are compositional differences of these minerals in the AOA CAIs and the relic CAIs in the PRCs. Pyroxenes in CAIs in AOAs are Al-diopsides, poor in TiO_2, Cr_2O_3 and MnO; the pyroxenes in the relic CAIs in PRCs are either Al-Ti-Cr-rich augites or Al-rich low-Ca pyroxenes (Tables 2 and 3; Figs. 3 and 4). Spinel grains in AOAs are Cr- and Ti-poor (Komatsu *et al.*, 2001), those in PRCs are Cr-Ti-rich (Table 6; Fig. 8a). Plagioclase grains in AOAs are pure anorthite (Komatsu *et al.*, 2001), those in the relic CAIs in PRCs contain detectable concentrations of Na_2O (Fig. 6a). (2) Most PRCs in CV chondrites contain abundant low-Ca pyroxene grains (Fig. 3a), whereas no low-Ca pyroxene was found in the CV AOAs (Fig. 3b). (3) Forsterite grains in AOAs have more ^{16}O-rich isotopic compositions (Hiyagon and Hashimoto, 1999; Krot and McKeegan, 2001) than those in Al-rich chondrules in ordinary chondrites (Russell *et al.*, 2000) and ferromagnesian chondrules in carbonaceous chondrites (Leshin *et al.*, 1998) studied so far. We note, however, that no O-isotopic compositions for the CV PRCs have yet been reported. (4) AOAs in the reduced CV chondrites show no evidence for being extensively melted; rather they are aggregates of solar nebula condensates that experienced high-temperature annealing (Komatsu *et al.*, 2001). In contrast, most PRCs experienced extensive melting. Based on these observations, we conclude that it is very unlikely that PRCs formed by melting of AOAs.

Comparison of Plagioclase-Rich Chondrules in the Reduced CV and CR Chondrites

Plagioclase-rich chondrules in the reduced CV chondrites share many features with those in CR chondrites (Krot and Keil, 2002). Similar to the CV PRCs, those in CR chondrites consist of magnesian low-Ca pyroxene and forsterite phenocrysts, FeNi-metal nodules, interstitial plagioclase, Al-Ti-Cr-rich low-Ca and high-Ca pyroxenes, and crystalline mesostasis composed of silica, plagioclase and augite. Two of the CR PRCs contain relic CAIs composed of anorthite, spinel, ±high-Ca pyroxene, and ±forsterite. Several PRCs in CR chondrites contain regions that are texturally and mineralogically similar to type I chondrules and consist of

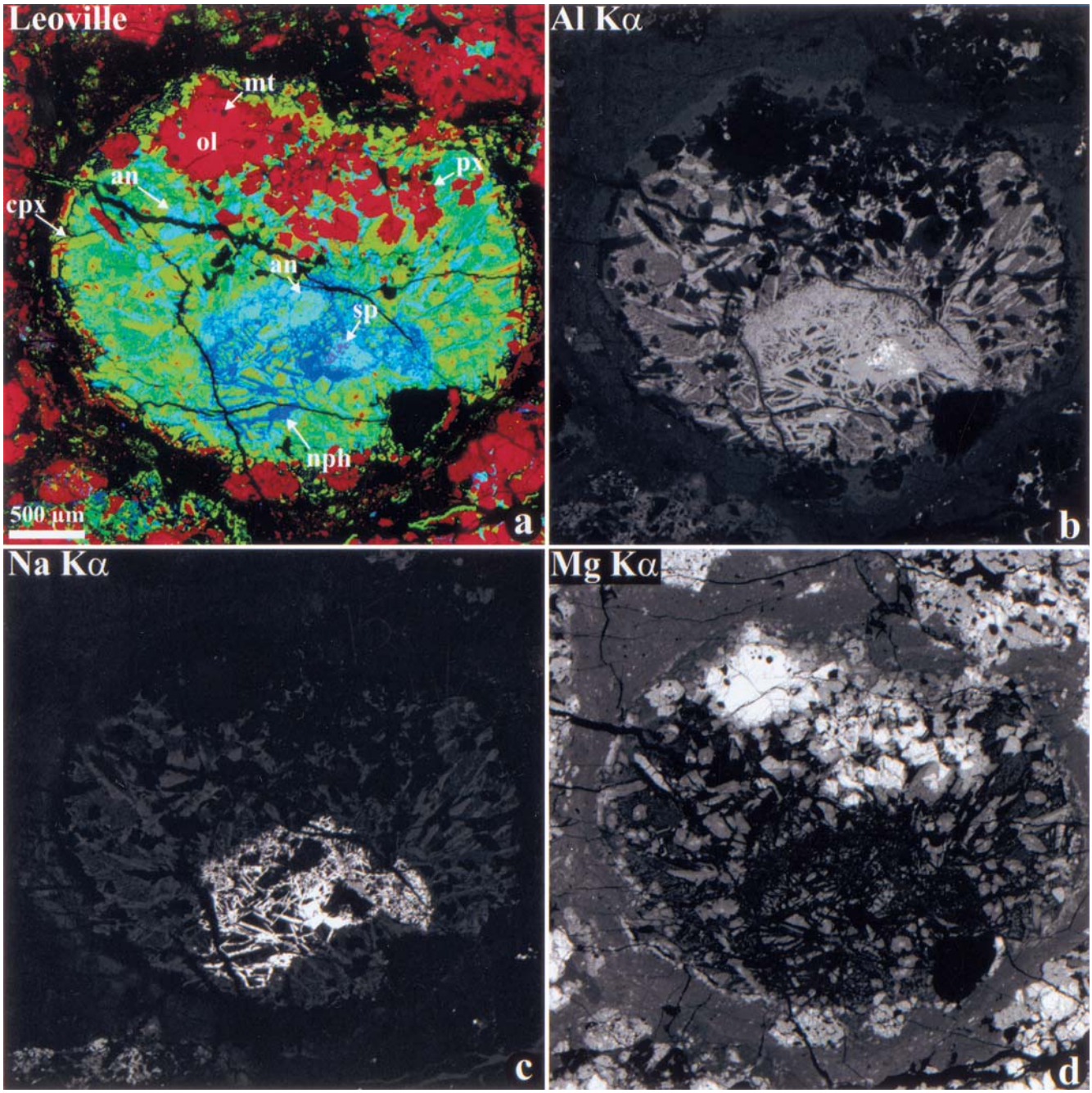

FIG. 16. Combined x-ray elemental map in Mg (red), Ca (green) and Al Kα (blue) (a), elemental maps in Al (b), Na (c) and Mg Kα x-rays (d) of PRC #1 in Leoville (1). Region outlined in (a) is shown in detail in (b); regions outlined and labeled in (b) are shown in detail in (c) and (d). The chondule consists of anorthite, interstitial elongated grains of low-Ca pyroxene overgrown by high-Ca pyroxenes and silica-rich crystalline mesostasis; it also contains a region composed of coarse-grained forsterite, low-Ca pyroxene and FeNi-metal nodules and a

forsterite, low-Ca pyroxene and abundant FeNi-metal nodules.

However, there are some differences between the CV and CR PRCs as well. (1) Plagioclase grains in the CR PRCs have peaks at higher contents of anorthite and MgO than those in the CV PRCs (Figs. 6 and 7). (2) Olivine grains in the CR PRCs have higher Cr_2O_3 contents and a narrower range in fayalite contents than those in the CV PRCs (Fig. 5). (3) The igneous rims around PRCs and compound PRCs were not found in CR chondrites; both types of objects are rather common in

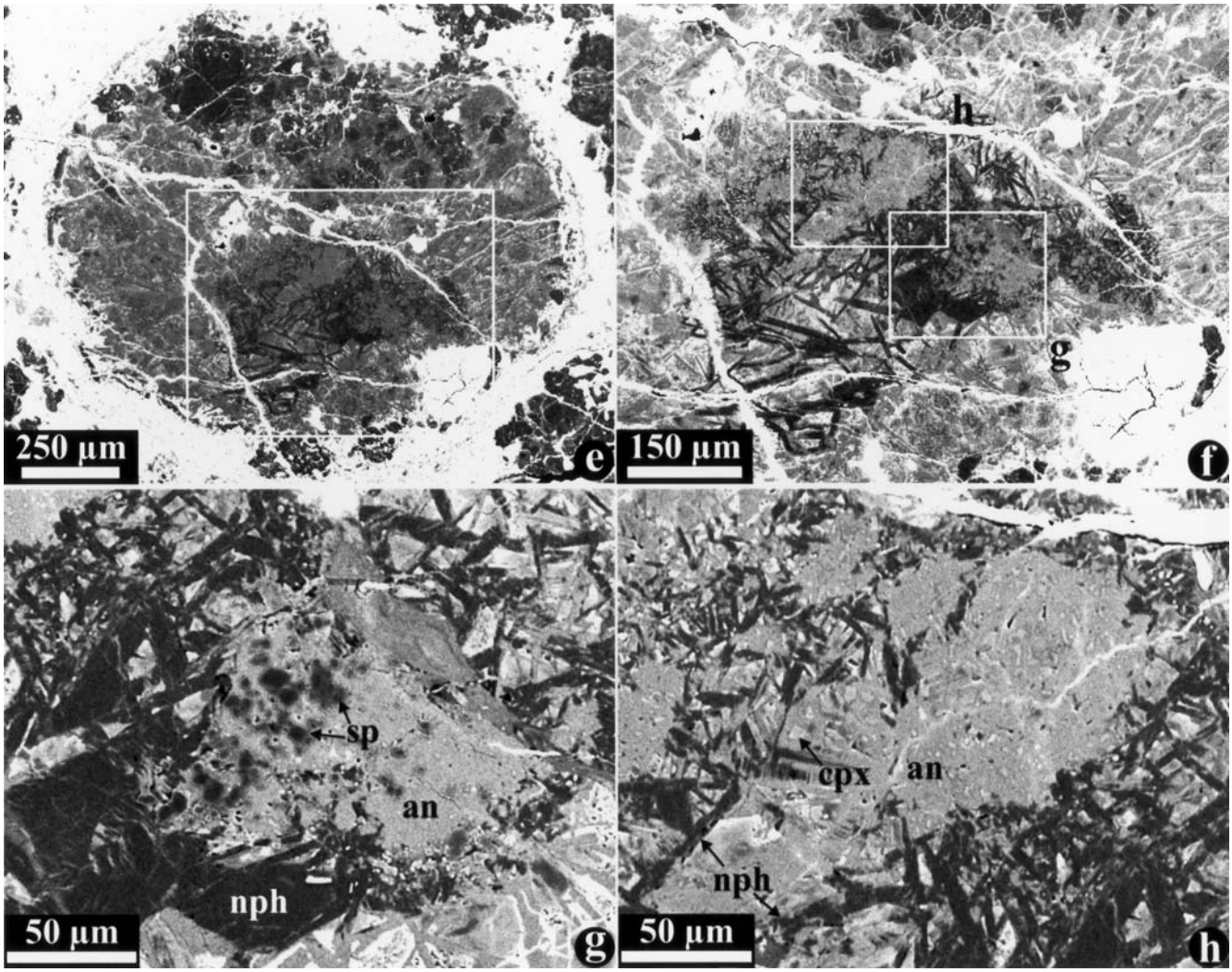

FIG. 16. *Continued.* Combined BSE images (e–h) of PRC #1 in Leoville (1). The chondule consists of anorthite, interstitial elongated grains of low-Ca pyroxene overgrown by high-Ca pyroxenes and silica-rich crystalline mesostasis; it also contains a region composed of coarse-grained forsterite, low-Ca pyroxene and FeNi-metal nodules and a rounded CAI composed of anorthite extensively replaced by nepheline and containing small inclusions of spinel.

CV chondrites. (4) Low-Ca pyroxene shells are rare around CR PRCs, but rather common around PRCs in CV chondrites. (5) Neither PRCs, nor relic CAIs in CR chondrites, show evidence for alteration. Most PRCs and many relic CAIs in PRCs in the reduced CV chondrites contain secondary nepheline and ferrosilite-hedenbergitic pyroxenes; secondary ferrous olivine was found in the Vigarano PRCs.

Some of the compositional differences listed above (*e.g.*, high fayalite contents in olivine and presence of secondary nepheline, hedenbergitic pyroxenes and ferrous olivine) are probably due to alteration that affected CAIs, chondrules, and matrices of the CV chondrites (MacPherson *et al.*, 1988; Kimura and Ikeda, 1995, 1997; Krot *et al.*, 1995, 1997, 1998a,b). The other differences (high Na content in plagioclase; presence of igneous rims) must be primary and indicate differences either in the formation history or the formation regions of PRCs in CR and CV chondrites (*e.g.*, number of recyclings, ambient nebular temperature, peak heating temperature, isolation temperature) or the compositions of their precursor materials. The higher Cr contents in forsterite phenocrysts in the CR PRCs compared to those in the CV PRCs may be a primary signature of the magnesian CR chondrule precursors (Weisberg *et al.*, 1995). Alternatively, chromium could have diffused out during very mild metamorphism in CV chondrites (*e.g.*, Hua *et al.*, 1988; Weinbruch *et al.*, 1990).

Based on these observations, we conclude that PRCs in the CV and CR chondrites formed in different chondrule-forming regions (*i.e.*, the CV and CR chondrule-forming regions, respectively). The common presence of relic CAIs having similar and the least refractory primary mineralogies (spinel,

anorthite, ±high-Ca pyroxenes) in PRCs from different chondrite groups (CV (this study), CR and CH (Krot and Keil, 2002), and CO (Jones and Brearley, 1994; Hutcheon and Jones, 1995; Jones and Hutcheon, 1996)) suggests that spinel-anorthite ± pyroxene CAIs were commonly present in the formation regions of PRCs. This may indicate that PRCs formed in a region intermediate between the regions where CAIs and ferromagnesian chondrules formed. This interpretation may explain the systematic enrichment in ^{16}O of ferromagnesian silicates (olivine and pyroxene) in Al-rich chondrules relative to those minerals in ferromagnesian chondrules (Russell *et al.*, 2000), because the gaseous reservoir in the CAI-forming region(s) was ^{16}O-enriched relative to the reservoir where ferromagnesian chondrules formed (Scott and Krot, 2001; Krot and McKeegan, 2001; McKeegan *et al.*, 2001). We note, however, that no oxygen isotope studies of the CV PRCs have yet been done.

The presence of independent compound PRCs and igneous rims around some of the PRCs in CV chondrites suggests that the CV PRC-forming regions experienced multiple heating episodes. It is interesting that evidence for recycling of CAIs (*e.g.*, presence of igneous, type B CAIs, presence of forsterite-bearing CAIs and relic CAIs inside CAIs) is relatively common in CV chondrites, but rare or not reported in other chondrite groups (*e.g.*, Blander and Fuchs, 1975; Dominik *et al.*, 1978; Clayton *et al.*, 1984; Wark *et al.*, 1987; MacPherson *et al.*, 1988; Weber and Bischoff, 1997; Russell *et al.*, 1998; Connolly and Burnett, 1999; Krot *et al.*, 2000a, 2001; El Goresy *et al.*, 2001). The presence of altered CAIs inside relatively unaltered host PRCs, the relatively high Ab contents in plagioclase of the CV PRCs and presence of sulfides in most of them may indicate that the last chondrule-forming process took place at low ambient temperature (~650 K) in the CV PRC-forming region. We cannot exclude, however, an asteroidal origin of sulfides in PRCs during mild parent-body metamorphism (*e.g.*, Grossman and Rubin, 1999).

Alteration of Plagioclase-Rich Chondrules and Relic Calcium-Aluminum-Rich Inclusions

Most plagioclase-rich chondrules in the reduced CV chondrites show evidence for Fe-Na-metasomatic alteration that resulted in the replacement of plagioclase by nepheline and sodalite, and of silica by ferrosilite-hedenbergitic pyroxenes (Fig. 1). This type of alteration is commonly observed in chondrules and CAIs of the Allende-like oxidized CV chondrites; it is less common in the reduced and Bali-like oxidized CV chondrites (*e.g.*, MacPherson *et al.*, 1988; Kimura and Ikeda, 1995, 1997; Krot *et al.*, 1995, 1997, 1998a,b). We note, however, that secondary ferrous olivine commonly observed in the Allende-like CV chondrites, where it replaces low-Ca pyroxenes and also occurs as thin rims around forsterite grains as haloes around FeNi-metal inclusions in forsterite (Hua *et al.*, 1988; Krot *et al.*, 1997), is very rare in the PRCs studied here. The secondary ferrous olivine was found in several PRCs in Vigarano, which is a breccia containing both the reduced and oxidized CV lithologies (Krot *et al.*, 2000b).

The nature of the CV alteration remains a controversial issue; two types of models, nebular (*e.g.*, Palme and Wark, 1988; Hua *et al.*, 1988; Palme and Fegley, 1990; Kimura and Ikeda, 1995) and asteroidal (*e.g.*, Kojima and Tomeoka, 1996; Krot *et al.*, 1995, 1998a,b), have been proposed. The presence of secondary feldspathoids and hedenbergitic pyroxenes in PRCs in the reduced CV chondrites indicates that even the latter are not completely unaltered meteorites. The alteration of most of the PRCs generally occurred from the outside, which is indicated by the higher abundance of feldspathoids in the chondrule peripheries and suggests that alteration (nebular or asteroidal) postdated chondrule solidification (Fig. 1).

There are, however, some important exceptions. The plagioclase-rich chondrule shown in Fig. 2g–j has a feldspathoid-rich core; several relic CAIs are more extensively altered than the host PRCs (Figs. 12–16). Similar alteration features, including extensive replacement of the plagioclase-spinel object (relic CAI?) by nepheline in the chondrule cores have been previously described in PRCs in the CO chondrites Kainsaz and Lance (Kurat and Kracher, 1980; Jones and Hutcheon, 1996). These observations and the relatively high abundance of sodium in plagioclase of the CV PRCs could be interpreted as a result of condensation of Na into chondrule precursors or chondrules of earlier generations (either as albitic plagioclase or as secondary feldspathoids) prior to chondrule formation (*i.e.*, in the nebula). This interpretation is consistent with a complex formation history in the nebula involving multiple stages of alteration and melting that has been previously invoked for a type B CAI in Vigarano by MacPherson and Davis (1993). We note however, that secondary feldspathoids in the relic CAIs in PRCs show no clear evidence for being affected by chondrule melting; delicate anorthite-feldspathoid textures show no evidence for melting or volatilization of feldspathoids; instead feldspathoids replace plagioclase. We speculate that anorthite of the relic objects may have been more susceptible to alteration than anorthitic plagioclase of the host chondrules.

Acknowledgements–We thank the Antarctic Meteorite Working Group (NASA, Johnson Space Center), the Smithsonian Institution (Washington, D.C.), and The Natural History Museum, London, for providing the polished thin sections of the meteorites studied here. We thank Rhian Jones, Makoto Kimura and Hiroko Nagahara for thoughtful reviews. This work was supported by NASA grants NAG 5-10610 (A. N. Krot, P. I.), NAG 5-4212 (K. Keil, P. I.) and work order W-18845 (I. Hutcheon, P. I.) and by Lawrence Livermore National Laboratory under the Laboratory Directed Research and Development (LDRD) program. Work performed under the auspices of the U.S. Department of Energy by Lawrence Livermore National Laboratory under contract W-7405-ENG-48. This is Hawaii Institute of Geophysics and Planetology publication No. 1194 and School of Ocean and Earth Science and Technology publication No. 5927.

Editorial handling: H. Nagahara

REFERENCES

BAR-MATTHEWS M., MACPHERSON G. J. AND GROSSMAN L. (1979) An SEM-petrographic study of amoeboid olivine aggregates in Allende (abstract). *Meteoritics* **14**, 342.

BISCHOFF A. AND KEIL K. (1984) Al-rich objects in ordinary chondrites: Related origin of carbonaceous and ordinary chondrites and their constituents. *Geochim. Cosmochim. Acta* **48**, 693–709.

BLANDER M. AND FUCHS L. H. (1975) Calcium-aluminum-rich inclusions in the Allende meteorite; evidence for a liquid origin. *Geochim. Cosmochim. Acta* **39**, 1605–1619.

BOSS A. P. (2001) Preservation of isotopic heterogeneity in the solar nebula (abstract). *Meteorit. Planet. Sci.* **36 (Suppl.)**, A26.

CLAYTON R. N., MACPHERSON G. J., HUTCHEON I. D., DAVIS A. M., GROSSMAN L., MAYEDA T. K., MOLINI-VELSKO C. A., ALLEN J. M. AND EL GORESY A. (1984) Two forsterite-bearing FUN inclusions in the Allende meteorite. *Geochim. Cosmochim. Acta* **48**, 535–548.

CONNOLLY H. C., JR. AND BURNETT D. S. (1999) A study of the minor element concentrations of spinels from two type B calcium-aluminum-rich inclusons: An investigation into potential formation conditions of calcium-aluminum-rich inclusions. *Meteorit. Planet. Sci.* **34**, 829–849.

CONNOLLY H. C., JR. AND LOVE S. G. (1998) The formation of chondrules; petrologic tests of the shock wave model. *Science* **280**, 62–67.

DOMINIK B., JESSBERGER E. K., STAUDACHER T., NAGEL K. AND EL GORESY A. (1978) A new type of white inclusion in Allende; petrography, mineral chemistry, ^{40}Ar-^{39}Ar ages, and genetic implications. *Proc. Lunar Planet. Sci. Conf.* **9th**, 1249–1266.

EL GORESY A., ZINNER E., MATSUNAMI S., PALME H., SPETTEL B., LIN Y. AND NASAROV M. A. (2001) Efremovka 101.1: A CAI with ultrarefractory REE patterns and enormous enrichments of Sc, Zr, and Y in fassaite and perovksite. *Geochim. Cosmochim. Acta* (in press).

FAGAN T. J., KROT A. N. AND KEIL K. (2000) Calcium-aAluminum-rich inclusions in enstatite chondrites (I): Mineralogy and textures. *Meteorit. Planet. Sci.* **35**, 771–783.

FAGAN T. J., MCKEEGAN K. D., KROT A. N. AND KEIL K. (2001) Calcium-aluminum-rich inclusions in enstatite chondrites (II): Oxygen isotopes. *Meteorit. Planet. Sci.* **36**, 223–230.

GOUNELLE M., SHU F. H., SHANG H., GLASSGOLD A. E., REHM K. E. AND LEE T. (2001) Extinct radioactivities and protosolar cosmic-rays: Self-shielding and light elements. *Astrophys. J.* **548**, 1051–1070.

GOSWAMI J. N. AND VANHALA H. A. T. (2000) Short-lived nuclides in the early solar system: Meteoritic evidence and plausible sources. In *Protostars and Planets IV* (eds. M. Mannings, A. P. Boss and S. S. Russell), pp. 963–994. Univ. Arizona Press, Tucson, Arizona, USA.

GOSWAMI J. N., SRINIVASAN G. AND ULYANOV A. A. (1994) Ion microprobe studies of Efremovka CAIs: I. Magnesium isotope composition. *Geochim. Cosmochim. Acta* **58**, 431–447.

GROSSMAN J. N. AND RUBIN A. E. (1999) The metamorphic evolution of matrix and opaque minerals in CO chondrites (abstract). *Lunar Planet. Sci.* **30**, #1639, Lunar and Planetary Institute, Houston, Texas, USA (CD-ROM).

GUAN Y., MCKEEGAN K. D. AND MACPHERSON G. J. (2000a) Oxygen isotopes of CAIs from unequilibrated enstatite chondrites: Characteristics and implications (abstract). *Lunar Planet. Sci.* **31**, #1744, Lunar and Planetary Institute, Houston, Texas, USA (CD-ROM).

GUAN Y., HUSS G. R., MACPHERSON G. J. AND WASSERBURG G. J. (2000b) Calcium-aluminum-rich inclusions from enstatite chondrites; indigenous or foreign? *Science* **289**, 1330–1333.

HIYAGON H. (2000) An ion microprobe study of oxygen isotopes in some inclusions in Kainsaz and Y-81020 CO3 chondrites (abstract). *NIPR Symp. Antarctic Meteorite* **25**, 19–21.

HIYAGON H. AND HASHIMOTO A. (1999) ^{16}O excesses in olivine inclusions in Yamato 86009 and Murchison chondrites and their relation to CAIs. *Science* **283**, 828–831.

HUA X., ADAM J., PALME H. AND EL GORESY A. (1988) Fayalite-rich rims veins, and halos around and in forsteritic olivines in CAIs and chondrules in carbonaceous chondrites: Types compositional profiles and constraints of their formation. *Geochim. Cosmochim. Acta* **52**, 1389–1408.

HSU W., HUSS G. R. AND WASSERBURG G. J. (2000) Compound CAI and muti-stage formation: Evidence of ^{26}Al abundances from the Allende 5241 CAI (abstract). *Lunar Planet. Sci.* **31**, #1734, Lunar and Planetary Institute, Houston, Texas, USA (CD-ROM).

HUSS G. R., MACPHERSON G. J., WASSERBURG G. J., RUSSELL S. S. AND SRINIVASAN G. (2001) Aluminium-26 in calcium-aluminium-rich inclusions and chondrules from unequilibrated ordinary chondrites. *Meteorit. Planet. Sci.* **36**, 975–999.

HUTCHEON I. D. AND HUTCHISON R. (1989) Evidence from the Semarkona ordinary chondrite for ^{26}Al heating of small planets. *Nature* **337**, 238–241.

HUTCHEON I. D. AND JONES R. H. (1995) The ^{26}Al-^{26}Mg record of chondrules; Clues to nebular chronology (abstract). *Lunar Planet. Sci.* **26**, 647–648.

HUTCHEON I. D., KROT A. N. AND ULYANOV A. A. (2000) ^{26}Al in anorthite-rich chondrules in primitive carbonaceous chondrites: Evidence chondrules post-date CAI (abstract). *Lunar Planet. Sci.* **31**, #1869, Lunar and Planetary Institute, Houston, Texas, USA (CD-ROM).

ITO M., YURIMOTO H. AND NAGASAWA H. (2000) A study of Mg and K isotopes in Allende CAIs: Implication to the time scale for the multiple heating processes (abstract). *Lunar Planet. Sci.* **31**, #1600, Lunar and Planetary Institute, Houston, Texas, USA (CD-ROM).

JONES R. H. AND BREARLEY A. (1994) Reduced, plagioclase-rich chondrules in the Lance and Kainsaz CO3 chondrites (abstract). *Lunar Planet. Sci.* **25**, 641–642.

JONES R. H. AND HUTCHEON I. D. (1996) Mineralogy and secondary alteration of a complex plagioclase-rich inclusion in Kainsaz (abstract). *Meteorit. Planet. Sci.* **31**, 67–68.

JONES R. H. AND SCOTT E. R. D. (1989) Petrology and thermal history of type IA chondrules in the Semarkona (LL3.0) chondrite. *Proc. Lunar Planet. Sci. Conf.* **19th**, 523–536.

JONES R. H., LEE T., CONNOLLY H. C., JR, LOVE S. G. AND SHANG H. (2000) Formation of chondrules and CAIs: Theory *vs.* Observation. In *Protostars and Planets IV* (eds. M. Mannings, A. P. Boss and S. S. Russell), pp. 927–962. Univ. Arizona Press, Tucson, Arizona, USA.

KIMURA M. AND IKEDA Y. (1995) Anhydrous alteration of Allende chondrules in the solar nebula. II: Alkali-Ca exchange reactions and formation of nepheline, sodalite and Ca-rich phases in chondrules. *Proc. NIPR Symp. Antarct. Meteorites* **8**, 123–138.

KIMURA M. AND IKEDA Y. (1997) Comparative study of anhydrous alteration of chondrules in reduced and oxidized CV chondrites. *Proc. NIPR Symp. Antarct. Meteorites* **10**, 191–202.

KITA N., NAGAHARA H., TOGASHI S. AND MORISHITA Y. (2000) A short duration of chondrule formation in the solar nebula; evidence from ^{26}Al in Semarkona ferromagnesian chondrules. *Geochim. Cosmochim. Acta* **64**, 3913–3922.

KOJIMA T. AND TOMEOKA K. (1996) Evidence for aqueous alteration and thermal metamorphism on the CV3 parent body: Microtextures of a dark inclusion from Allende. *Geochim. Cosmcohim. Acta* **60**, 2651–2666.

KOMATSU M., KROT A. N., PETAEV M. I., ULYANOV A. A., KEIL K. AND MIYAMOTO M. (2001) Mineralogy and petrography of amoeboid olivine aggregates from the reduced CV3 chondrites Efremovka, Leoville and Vigarano: Products of nebular condensation, accretion and annealing. *Meteorit. Planet. Sci.* **36**, 629–643.

KRING D. A. AND BOYNTON W. V. (1990) Trace-element compositions of Ca-rich chondrules from Allende: Relationships between refractory inclusions and ferromagnesian chondrules (abstract). *Meteoritics* **25**, 377.

KRING D. A. AND HOLMEN B. A. (1988) Petrology of anorthite-rich chondrules in CV3 and CO3 chondrites (abstract). *Meteoritics* **23**, 282.

KROT A. N. (2000) Anorthite-rich chondrules from primitive carbonaceous chondrites: Genetic links between CAI and chondrules (abstract). *Meteorit. Planet. Sci.* **35 (Suppl.)**, A93.

KROT A. N. AND KEIL K. (2002) Anorthite-rich chondrules in CR and CH carbonaceous chondrites: Genetic link between calcium-aluminum-rich inclusions and ferromagnesian chondrules. *Meteorit. Planet. Sci.* **37**, 91–111.

KROT A. N. AND WASSON J. T. (1995) Igneous rims on FeO-rich and FeO-poor chondrules in ordinary chondrites. *Geochim. Cosmochim. Acta* **59**, 4951–4966.

KROT A. N. AND MCKEEGAN K. D. (2001) Oxygen-isotopic compositions of forsterite in an accretionary rim around calcium-aluminum-rich inclusion and in an amoeboid olivine aggregate from the reduced CV chondrite Efremovka and their significance (abstract). *Lunar Planet. Sci.* **32**, #2016, Lunar and Planetary Institute, Houston, Texas, USA (CD-ROM).

KROT A. N., SCOTT E. R. D. AND ZOLENSKY M. E. (1995) Mineralogic and chemical variations among CV3 chondrites and their components: Nebular and asteroidal processing. *Meteoritics* **30**, 748–775.

KROT A. N., SCOTT E. R. D. AND ZOLENSKY M. E. (1997) Origin of fayalitic olivine rims and lath-shaped matrix olivine in the CV3 chondrite Allende and its dark inclusions. *Meteorit. Planet. Sci.* **32**, 31–49.

KROT A. N., PETAEV M. I., SCOTT E. R. D., CHOI B-G., ZOLENSKY M. E. AND KEIL K. (1998a) Progressive alteration in CV3 chondrites: More evidence for asteroidal alteration. *Meteorit. Planet. Sci.* **33**, 1065–1085.

KROT A. N., PETAEV M. I., ZOLENSKY M. E., KEIL K., SCOTT E. R. D. AND NAKAMURA K. (1998b) Secondary calcium-iron-rich minerals in the Bali-like and Allende-like oxidized CV3 chondrites and Allende dark inclusions. *Meteorit. Planet. Sci.* **33**, 623–645.

KROT A. N., SAHIJPAL S., MCKEEGAN K. D., WEBER D., GRESHAKE A, ULYANOV A. A., HUTCHEON I. D. AND KEIL K. (1999) Mineralogy, Al-Mg and oxygen isotope studies of the relic CAIs in chondrules (abstract). *Meteorit. Planet. Sci.* **34 (Suppl.)**, A68–A69.

KROT A. N., ULYANOV A. A. AND KEIL K. (2000a) Forsterite-bearing Ca,Al-rich inclusion from the reduced CV chondrite Efremovka (abstract). *Meteorit. Planet. Sci.* **35 (Suppl.)**, A93–A94.

KROT A. N., MEIBOM A. AND KEIL K. (2000b) A clast of Bali-like oxidized CV3 material in the reduced CV3 chondrite breccia Vigarano. *Meteorit. Planet. Sci.* **35**, 817–827.

KROT A. N., MCKEEGAN K. D., RUSSELL S. S., MEIBOM A., WEISBERG M. K., ZIPFEL J., KROT T. V., FAGAN T. J. AND KEIL K. (2001) Refractory Ca, Al-rich inclusions and Al-diopside-rich chondrules in the metal-rich chondrites Hammadah al Hamra 237 and QUE 94411. *Meteorit. Planet. Sci.* **36**, 1189–1217.

KURAT G. AND KRACHER A. (1980) Basalts in the Lance carbonaceous chondrite. *Zeitschr. Naturforsch.* **35A**, 180–190.

LEE T., PAPANASTASSIOU D. A. AND WASSERBURG G. J. (1976) Demonstration of ^{26}Mg excess in Allende and evidence for ^{26}Al. *Geophys. Res. Lett.* **3**, 41–44.

LESHIN L. A., MCKEEGAN K. D., ENGRAND C., ZANDA B., BOUROT-DENISE M. AND HEWINS R. H. (1998) Oxygen-isotopic studies of isolated and chondrule olivine from Renazzo and Allende (abstract). *Meteorit. Planet. Sci.* **33 (Suppl.)**, A93–A94.

MACPHERSON G. J. AND DAVIS A. M. (1993) A petrologic and ion microprobe study of a Vigarano Type B refractory inclusion: Evolution by multiple stages of alteration and melting. *Geochim. Cosmochim. Acta* **57**, 231–243.

MACPHERSON G. J., WARK D. A. AND ARMSTRONG J. T. (1988) Primitive material surviving in chondrites: Refractory inclusions. In *Meteorites and the Early Solar System* (eds. J. F. Kerridge and M. S. Matthews), pp. 746–807. Univ. Arizona Press, Tucson, Arizona, USA.

MACPHERSON G. J., DAVIS A. M. AND ZINNER E. K. (1995) The distribution of aluminum-26 in the early solar system: A reappraisal. *Meteoritics* **30**, 365–386.

MARHAS K. K., HUTCHEON I. D., KROT A. N. AND GOSWAMI J. N. (2000) ^{26}Al in carbonaceous chondrite chondrules (abstract). *Meteorit. Planet. Sci.* **35 (Suppl.)**, A102.

MARUYAMA S., YURIMOTO H. AND SUENO S. (1998a) CAI related spinel in a compound chondrule: Evidence of O isotope (abstract). *Lunar Planet. Sci.* **29**, #1342, Lunar and Planetary Institute, Houston, Texas, USA (CD-ROM).

MARUYAMA S., YURIMOTO H. AND SUENO S. (1998b) Spinel-bearing chondrules in the Allende meteorite (abstract). *Meteorit. Planet. Sci.* **33 (Suppl.)**, A98.

MCKEEGAN K. D., LESHIN L. A., RUSSELL S. S. AND MACPHERSON G. J. (1998) Oxygen isotope abundances in calcium-aluminum-rich inclusions from ordinary chondrites: Implications for nebular heterogeneity. *Science* **280,** 414–418.

MCKEEGAN K. D., GREENWOOD J. P., LESHIN L. A. AND COZARINSKY M. (2000a) Abundance of ^{26}Al in ferromagnesian chondrules of unequilibrated ordinary chondrites (abstract). *Lunar Planet. Sci.* **31**, #2009, Lunar and Planetary Institute, Houston, Texas, USA (CD-ROM).

MCKEEGAN K. D., CHAUSSIDON M. AND ROBERT F. (2000b) Incorporation of short-lived ^{10}Be in a calcium-aluminum-rich inclusion from the Allende meteorite. *Science* **289**, 1334–1337.

MCKEEGAN K. D., KROT A. N. AND SCOTT E. R. D. (2001) Variable oxygen isotopic compositions of gaseous reservoirs: Clues to the formation of CAIs and chondrules (abstract). *Meteorit. Planet. Sci.* **36 (Suppl.)**, A129.

MISAWA K. AND NAKAMURA N. (1988) Highly fractionated rare-earth elements in ferromagnesian chondrules from the Felix (CO3) meteorite. *Nature* **334**, 47–49.

MISAWA K. AND NAKAMURA N. (1996) Origin of refractory precursor components of chondrules from carbonaceous chondrites. In *Chondrules and the Protoplanetary Disk* (eds. R. H. Hewins, R. H. Jones and E. R. D. Scott), pp. 99–105. Cambridge Univ. Press, New York, New York, USA.

MOSTEFAOUI S., KITA N. T., NAGAHARA H., TOGASHI S. AND MORISHITA Y. (1999) Aluminum-26 in two ferromagnesian chondrules from a highly unequilibrated ordinary chondrite: Evidence of a short period of chondrule formation (abstract). *Meteorit. Planet. Sci.* **34 (Suppl.)**, A84.

PALME H. AND FEGLEY B., JR. (1990) High-temperature condensation of iron-rich olivine in the solar nebula. *Earth Planet. Sci. Lett.* **101**, 180–195.

PALME H. AND WARK D. A. (1988) CV-chondrites: High-temperature gas-solid equilibrium *vs.* parent body metamorphism (abstract). *Lunar Planet. Sci.* **19**, 897–898.

PODOSEK F. A. AND CASSEN P. (1994) Theoretical, observational, and isotopic estimates of the lifetime of the solar nebula. *Meteoritics* **29**, 6–25.

RUBIN A. (1984) Coarse-grained chondrule rims in type 3 chondrites. *Geochim. Cosmochim. Acta* **48**, 1779–1789.

RUBIN A. E. (2000) Petrologic, geochemical and experimental constraints on models of chondrule formation. *Earth Sci. Rev.* **50**, 3–27.

RUBIN A. E. AND KROT A. N. (1996) Multiple heating of chondrules. In *Chondrules and the Protoplanetary Disk* (eds. R. H. Hewins, R. H. Jones and E. R. D. Scott), pp. 173–180. Cambridge Univ. Press, New York, New York, USA.

RUSSELL S. S., SRINIVASAN G., HUSS G. R., WASSERBURG G. J. AND MACPHERSON G. J. (1996) Evidence for wide spread ^{26}Al in the solar nebula and constraints for nebula time scales. *Science* **273**, 757–762.

RUSSELL S. S., HUSS G. R., MACPHERSON G. J. AND WASSERBURG G. J. (1997) Early and late chondrule formation: New constraints for solar nebula chronology from ^{26}Al/^{27}Al in unequilibrated ordinary chondrites (abstract). *Lunar Planet. Sci.* **28**, 1209–1210.

RUSSELL S. S., HUSS G. R., FAHEY A. J., GREENWOOD R. C., HUTCHISON R. AND WASSERBURG G. J. (1998) An isotopic and petrologic study of calcium-aluminum-rich inclusions from CO3 meteorites. *Geochim. Cosmochim. Acta* **62**, 689–714.

RUSSELL S. S., MACPHERSON G. J., LESHIN L. A. AND MCKEEGAN K. D. (2000) ^{16}O enrichments in aluminum-rich chondrules from ordinary chondrites. *Earth Planet. Sci. Lett.* **184**, 57–74.

SAHIJPAL S., GOSWAMI J. N., DAVIS A. M., GROSSMAN L. AND LEWIS R. S. (1998) A stellar origin for the short-lived nuclides in the early solar system. *Nature* **391**, 559–561.

SCOTT E. R. D. AND KROT A. N. (2001) Oxygen isotopic compositions and origins of calcium-aluminum-rich inclusions and chondrules. *Meteorit. Planet. Sci.* **36**, 1307–1319.

SHENG Y. J., HUTCHEON I. D. AND WASSERBURG G. J. (1991) Origin of plagioclase-olivine inclusions in carbonaceous chondrites. *Geochim. Cosmochim. Acta* **55**, 581–599.

SHU F. H., SHANG H. AND LEE T. (1996) Toward an astrophysical theory of chondrites. *Science* **271**, 1545–1552.

SHU F. H., SHANG H., GLASSGOLD A. E. AND LEE T. (1997) X-rays and fluctuating x-winds from protostars. *Science* **277**, 1475–1479.

SHU F. H., SHANG H., GOUNELLE M., GLASSGOLD A. E. AND LEE T. (2001) The origin of chondrules and refractory inclusions in chondritic meteorites. *Astrophys. J.* **548**, 1029–1070.

SRINIVASAN G., RUSSELL S. S., MACPHERSON G. J., HUSS G. R. AND WASSERBURG G. J. (1996a) New evidence for ^{26}Al in CAI and chondrules from type 3 ordinary chondrites (abstract). *Lunar Planet. Sci.* **27**, 1257–1258.

SRINIVASAN G., SAHIJAPAL S., ULYANOV A. A. AND GOSWAMI J. N. (1996b) Ion microprobe studies of Efremovka CAIs: II. Potassium isotope composition and ^{41}Ca in the early solar system. *Geochim. Cosmochim. Acta* **60**, 1823–1835.

VANHALA H. A. T. AND BOSS A. P. (2000) Injection of radioactivities into the forming solar system (abstract). *Lunar Planet. Sci.* **31**, #1061, Lunar and Planetary Institute, Houston, Texas, USA (CD-ROM).

WADHWA M. AND RUSSELL S. S. (2000) Timescales of accretion and differentiation in the early solar system: The meteoritic evidence. In *Protostars and Planets IV* (eds. V. M. Mannings, A. P. Boss and S. S. Russell), pp. 995–1018. Univ. Arizona Press, Tucson, Arizona, USA.

WARK D. A., BOYNTON W. V., KEAYS R. R. AND PALME H. (1987) Trace element and petrologic clues to the formation of forsterite-bearing Ca-Al-rich inclusions in the Allende meteorite. *Geochim. Cosmochim. Acta* **51**, 607–622.

WASSON J. T., KROT A. N., LEE M. S. AND RUBIN A. E (1994) Compound chondrules in ordinary chondrites: Evidence for multiple heating events and for large-scale heterogenieties in the nebula. *Geochim. Cosmochim. Acta* **59**, 1847–1869.

WEBER D. AND BISCHOFF A. (1997) Refractory inclusions in the CR chondrite Acfer 059—El Djouf 001: Petrology, chemical composition, and relationship to inclusion populations in other types of carbonaceous chondrites. *Chem. Erde* **57**, 1–24.

WEINBRUCH S., PALME H., MÜELLER W. F. AND EL GORESY A. (1990) FeO-rich rims and veins in Allende forsterite; evidence for high-temperature condensation at oxidizing conditions. *Meteoritics* **25**, 115–125.

WEISBERG M. K., PRINZ M., CLAYTON R. N., MAYEDA T. K., GRADY M. M. AND PILLINGER C. T. (1995) The CR chondrite clan. *Proc. NIPR Symp. Antarctic Meteorites* **8**, 11–32.

WOOD J. A. (1996) Unresolved issues in the formation of chondrules and chondrites. In *Chondrules and the Protoplanetary Disk* (eds. R. H. Hewins, R. H. Jones and E. R. D. Scott), pp. 55–71. Cambridge Univ. Press, New York, New York, USA.

WOOD J. A. (1998a) Constraints placed by aluminum-26 on early solar system history (abstract). *Meteorit. Planet. Sci.* **33 (Suppl.)**, A168–A169.

WOOD J. A. (1998b) Meteoritic evidence for the infall of large interstellar dust aggregates during the formation of the solar system. *Astrophys. J.* **503**, L101–L104.